



# Paired $\delta^{13}\text{C}_{\text{carb}}$ and $\delta^{13}\text{C}_{\text{org}}$ records of Upper Ordovician (Sandbian–Katian) carbonates in North America and China: Implications for paleoceanographic change

Seth A. Young<sup>a,\*</sup>, Matthew R. Saltzman<sup>a</sup>, Stig M. Bergström<sup>a</sup>, Stephen A. Leslie<sup>b</sup>, Chen Xu<sup>c</sup>

<sup>a</sup> Division of Geological Sciences, School of Earth Sciences, the Ohio State University, 275 Mendenhall Laboratory, 125 S. Oval Mall, Columbus, OH 43210, USA

<sup>b</sup> Department of Geology and Environmental Science, James Madison University, MSC 6903, Harrisonburg, VA 22807, USA

<sup>c</sup> State Key Laboratory of Palaeobiology and Stratigraphy, Nanjing Institute of Geology and Palaeontology, Chinese Academy of Sciences, 39 East Beijing Road, Nanjing 210008, People's Republic of China

## ARTICLE INFO

### Article history:

Received 6 February 2008

Received in revised form 16 August 2008

Accepted 15 September 2008

### Keywords:

Late Ordovician

Katian

Carbon isotopes

Organic carbon

Water masses

Carbon dioxide

## ABSTRACT

Late Sandbian–Early Katian marine carbonates from two sections in North America and one in south China were analyzed for paired  $\delta^{13}\text{C}_{\text{carb}}$  and  $\delta^{13}\text{C}_{\text{org}}$ , and revealed similar  $\delta^{13}\text{C}_{\text{carb}}$  but varying trends in  $\delta^{13}\text{C}_{\text{org}}$  stratigraphy while all sections recorded a well-known positive  $\delta^{13}\text{C}_{\text{carb}}$  shift. These  $\delta^{13}\text{C}_{\text{org}}$  records are the first through the Guttenberg  $\delta^{13}\text{C}_{\text{carb}}$  excursion (GICE) in China, Oklahoma, and West Virginia. In south China a positive excursion in  $\delta^{13}\text{C}_{\text{org}}$  is associated with the latter part of the positive  $\delta^{13}\text{C}_{\text{carb}}$  excursion and closely resembles trends from Iowa and Pennsylvania that have been interpreted to reflect a lowering of atmospheric  $p\text{CO}_2$  levels. The  $\delta^{13}\text{C}_{\text{org}}$  trends from Oklahoma and West Virginia differ significantly from what is observed in China. This likely indicates that local changes in nutrient cycling and phytoplankton growth rates were the dominant control on  $^{12}\text{C}$  fractionation in Oklahoma and West Virginia, masking a possible global signal of lowered atmospheric  $p\text{CO}_2$  levels observed in China.

© 2008 Elsevier B.V. All rights reserved.

## 1. Introduction

It is widely accepted that the Hirnantian Stage (445–443 Ma) of the Ordovician period was a time of major global environmental changes that culminated in the re-emergence of large continental ice sheets over polar landmasses (Brenchley et al., 1994). However, the circumstances surrounding the initiation of the Hirnantian climate transition remains controversial, and it has been suggested that the Late Ordovician ice age climate actually began ~10 m. y. prior in the Katian Stage (e.g., Frakes et al., 1992; Pope and Steffen, 2003; Saltzman and Young, 2005). In addition to lithological and biological indicators, an important line of evidence that is consistent with global cooling beginning as early as the Katian is a positive  $\delta^{13}\text{C}$  excursion in marine carbonates ( $\delta^{13}\text{C}_{\text{carb}}$ ) (e.g., Ludvigson et al., 1996; Patzkowsky et al., 1997; Ainsaar et al., 1999; Young et al., 2005). This  $\delta^{13}\text{C}_{\text{carb}}$  excursion is commonly interpreted to reflect enhanced burial of organic carbon on a global scale. Furthermore, the positive  $\delta^{13}\text{C}_{\text{carb}}$  excursion in the early Katian is also associated with an even larger positive shift in organic matter isotopes ( $\delta^{13}\text{C}_{\text{org}}$ ) (Hatch et al., 1987; Ludvigson et al., 1996; Patzkowsky et al., 1997). This decreased isotopic difference between  $\delta^{13}\text{C}_{\text{carb}}$  and  $\delta^{13}\text{C}_{\text{org}}$  ( $\Delta^{13}\text{C} = \delta^{13}\text{C}_{\text{carb}} - \delta^{13}\text{C}_{\text{org}}$ ) has been interpreted to

reflect a fall in  $p\text{CO}_2$  (and  $\text{CO}_{2(\text{aq})}$ ) below a critical threshold for ice-sheet growth in the Late Ordovician (Patzkowsky et al., 1997; Herrmann et al., 2003, 2004).

Unlike the widely studied  $\delta^{13}\text{C}_{\text{carb}}$  excursion in the Katian, the  $\delta^{13}\text{C}_{\text{org}}$  trend has not been globally documented. Paired analysis of  $\delta^{13}\text{C}_{\text{carb}}$  and  $\delta^{13}\text{C}_{\text{org}}$  in many different regions is critical because the isotopic difference between  $\delta^{13}\text{C}_{\text{carb}}$  and  $\delta^{13}\text{C}_{\text{org}}$  ( $\Delta^{13}\text{C}$ ) is known to respond to variables other than  $p\text{CO}_2$ , such as phytoplankton growth rates, cell geometries (volume to surface area ratios), and the biological source of the organic matter preserved (Francois et al., 1993; Hinga et al., 1994; Bidigare et al., 1997; Popp et al., 1998). Furthermore, in the case of the early Katian, the epeiric sea water masses that flooded landmasses have been shown to vary in critical parameters (i.e., nutrient concentrations) that affect growth rates and algal ecology (e.g., Holmden et al., 1998; Young et al., 2005; Panchuk et al., 2006).

Presented here are paired analyses of  $\delta^{13}\text{C}_{\text{carb}}$  and  $\delta^{13}\text{C}_{\text{org}}$  from several Late Ordovician (late Sandbian to early Katian Stage) carbonate sections in China and North America (Fig. 1) that can be correlated to previously studied sections using biostratigraphy and/or K-bentonite event stratigraphy. The documented  $\Delta^{13}\text{C}$  trends are evaluated alongside with previously published data (Patzkowsky et al., 1997; Pancost et al., 1999) in the context of fluctuating local paleoceanographic conditions during an episode of global environmental change in the Late Ordovician. Our results reveal evidence of local and also what may be global carbon cycle effects on  $\delta^{13}\text{C}$  in different sections,

\* Corresponding author. Present address: Department of Geological Sciences, Indiana University, Bloomington, IN 47405, USA.

E-mail addresses: [young.899@osu.edu](mailto:young.899@osu.edu), [seayoung@indiana.edu](mailto:seayoung@indiana.edu) (S.A. Young).

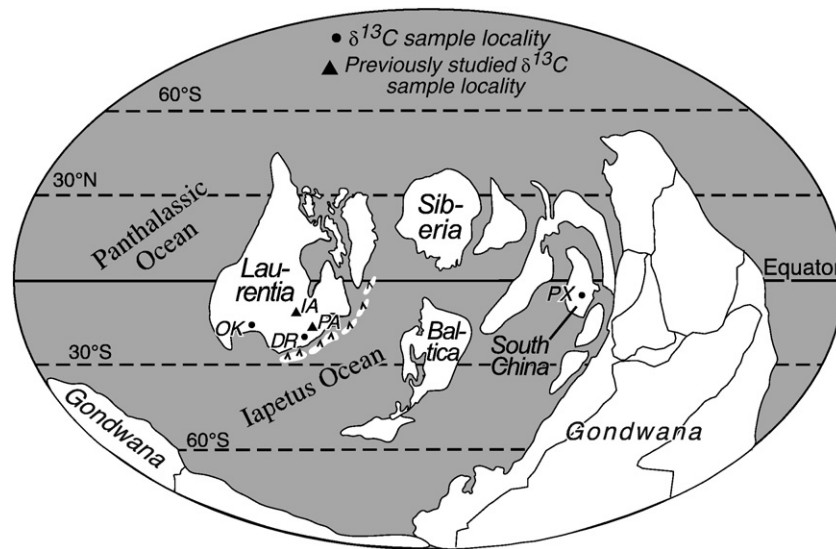


**Fig. 1.** Katian (Upper Ordovician) paleogeographic reconstruction (modified from Witzke, 1990; Scotese and McKerrow, 1991) showing locations of our study sections in Oklahoma (OK), West Virginia (DR), and southeast China (PX) along with sections previously investigated for paired  $\delta^{13}\text{C}_{\text{carb}}$  and  $\delta^{13}\text{C}_{\text{org}}$  analyses from Iowa (IA) and Pennsylvania (PA) (Ludvigson et al., 1996; Patzkowsky et al., 1997; Pancost et al., 1999).

and emphasize the importance of continued high-resolution study of paired  $\delta^{13}\text{C}_{\text{carb}}$  and  $\delta^{13}\text{C}_{\text{org}}$  trends in widely separated oceanic regions.

## 2. Geologic background

Recent work by the International Subcommittee on Ordovician Stratigraphy (ISOS) has led to the division of the Upper Ordovician Series into three globally classified stages, in ascending order, Sandbian, Katian, and Hirnantian (Bergström et al., 2000). Katian epeiric sea deposits of North America record regional extinctions of marine benthos and a distinct change in the style of carbonate deposition (“tropical-type” to “temperate-type”) (e.g., Patzkowsky and Holland, 1993; Holland and Patzkowsky, 1996; Patzkowsky et al., 1997; Pope and Read, 1998; Pope and Steffen, 2003). The associated positive  $\delta^{13}\text{C}_{\text{carb}}$  shift, known as the Guttenberg carbon isotope excursion (GICE), is the most widely documented excursion in the Upper Ordovician outside of the Hirnantian. The GICE has been documented in marine limestones from numerous localities in North America, Europe, and recently in Asia (Fig. 1) (e.g., Ludvigson et al., 1996; Patzkowsky et al., 1997; Ainsaar et al., 1999; Bergström et al., in press). As a result of intensive study of the GICE over a wide area of North America, it has been possible to observe local variations in the magnitude of the excursion that are linked to differences in paleoceanographic setting and nutrient cycling (e.g., Holmden et al., 1998; Young et al., 2005; Panchuk et al., 2006).

The GICE begins near the *Phragmodius undatus*/*Plectodina tenuis* Midcontinent conodont zonal boundary, and ends near the *P. tenuis*/*Belodina confluens* zonal boundary (Young et al., 2005). The GICE lies within the upper part of the *Amorphognathus tvaerensis* North Atlantic conodont zone, and falls within the North American *Corynoides americanus* and *Orthograptus ruedemanni* graptolite zones (Saltzman et al., 2003). These zones comprise the lower part of the newly defined *Diplacanthograptus caudatus* Graptolite Biozone, which marks the base of the Katian Global Stage of the Upper Ordovician (Goldman et al., 2007). This positive  $\delta^{13}\text{C}_{\text{carb}}$  excursion has also been shown to begin several meters above widespread altered volcanic ash beds, known as the Millbrig and Kinnekulle K-bentonites in eastern North America and Baltoscandia, respectively (Ainsaar et al., 1999; Saltzman et al., 2003; Young et al., 2005).

The positive  $\delta^{13}\text{C}_{\text{org}}$  excursion of up to +7.5‰, associated with the GICE, has been documented from two North American sections in Iowa and Pennsylvania (Hatch et al., 1987; Ludvigson et al., 1996;

Patzkowsky et al., 1997). Our new paired  $\delta^{13}\text{C}_{\text{carb}}$  and  $\delta^{13}\text{C}_{\text{org}}$  curves include sections through (1) the Pagoda Formation, near Yichang City (Hubei Province) in south-central China; (2) the Bromide and Viola Springs formations near Fittstown (Pontotoc County), Oklahoma, USA; and (3) the Nealmont and Dolly Ridge formations, near Riverton (Pendleton County), West Virginia, USA. Previous work on conodonts and graptolite biostratigraphy, sequence and event stratigraphy, and  $\delta^{13}\text{C}_{\text{carb}}$  stratigraphy of these three sections allow us to correlate the three sections to other studied regions (Perry, 1972; Alberstadt, 1973; Sweet, 1983; Finney, 1986; An, 1987; Keith, 1989; Chen et al., 1995; Young et al., 2005; Goldman et al., 2007; Bergström et al., in press).

The recognition of upper *P. undatus* through lower *B. confluens* Midcontinent Conodont Zones and upper *C. bicornis* through lower *C. spiniferus* Graptolite Zones from the Bromide and Viola Springs formations at the Fittstown, Oklahoma section (Sweet, 1983; Finney, 1986; Goldman et al., 2007) allows for a unique and definitive biostratigraphic framework for the  $\delta^{13}\text{C}$  stratigraphy presented here. Based upon the limited biostratigraphic studies conducted on the Dolly Ridge Formation, West Virginia, the formation lies within the upper *P. undatus* through basal *B. confluens* Conodont Zones (Keith, 1989; Young et al., 2005). The presence of a prominent altered volcanic ash bed (Deicke K-bentonite) several meters below the beginning of the GICE in both the Oklahoma and West Virginia sections supports the conodont biostratigraphic correlations (Young et al., 2005; Goldman et al., 2007).

Additionally the GICE has been demonstrated to occur above the M4–M5 sequence stratigraphic boundary in Eastern North America (Young et al., 2005), and this boundary represents a major sea level rise and transition from “tropical-type” to “temperate-type” carbonate deposition style (Holland and Patzkowsky, 1996). The *P. undatus* through lower *B. confluens* Conodont Zones have been previously recognized in the Salona and Coburn formations of central Pennsylvania (Valek, 1982; Richardson and Bergström, 2003), which facilitates the correlation of the Patzkowsky et al. (1997) paired  $\delta^{13}\text{C}$  stratigraphy with the new data presented here.

The North Atlantic conodont fauna of the Pagoda Formation in south-central China can be well correlated with conodonts from Baltoscandia, specifically the conodonts *Hamarodus europaeus* and *Amorphognathus* aff. *Am. ventilatus* that appear in the same intervals of the GICE as documented previously in Estonia (Männik and Vira, 2005; Bergström et al., in press). Based upon previous studies of integrated biostratigraphy (conodonts, graptolites, chitinozoans),

**Table 1**  
Stable Isotope data, Puxihe Quarry, Hubei Province, China

Meters <sup>a</sup>	$\delta^{13}\text{C}_{\text{carb}}$	$\delta^{13}\text{C}_{\text{org}}$	%TOC <sup>b</sup>	Conodont Zone	Formation
0.00	0.70	-29.11	0.063	<i>Am. tvaerensis</i>	Pagoda
0.25	1.06	-29.55	0.070	<i>Am. tvaerensis</i>	Pagoda
0.50	1.22	-28.96	0.056	<i>Am. tvaerensis</i>	Pagoda
1.00	1.70	-28.50	0.047	<i>Am. tvaerensis</i>	Pagoda
1.50	1.39	-29.06	0.047	<i>Am. tvaerensis</i>	Pagoda
2.00	2.41	-28.66	0.043	<i>Am. tvaerensis</i>	Pagoda
2.50	2.11	-28.47	0.032	<i>Am. tvaerensis</i>	Pagoda
3.00	2.19	-28.88	0.034	<i>Am. tvaerensis</i>	Pagoda
3.25	2.35	-28.86	0.032	<i>Am. tvaerensis</i>	Pagoda
3.50	2.01	-29.37	0.074	<i>Am. tvaerensis</i>	Pagoda
3.75	1.88	-27.42	0.029	<i>Am. tvaerensis</i>	Pagoda
4.00	1.94	-27.61	0.046	<i>Am. tvaerensis</i>	Pagoda
4.25	1.60	-26.75	0.032	<i>Am. tvaerensis</i>	Pagoda
4.50	1.74	-27.30	0.037	<i>Am. tvaerensis</i>	Pagoda
5.00	1.52	-26.90	0.029	<i>Am. tvaerensis</i>	Pagoda
5.50	1.82	-28.11	0.027	<i>Am. tvaerensis</i>	Pagoda
5.75	1.62	-28.34	0.051	<i>Am. tvaerensis</i>	Pagoda
6.00	1.39	-28.57	0.034	<i>Am. tvaerensis</i>	Pagoda
6.50	1.40	-27.95	0.043	<i>Am. tvaerensis</i>	Pagoda
7.00	1.20	-27.83	0.035	<i>Am. tvaerensis</i>	Pagoda
8.00	1.24	-27.82	0.030	<i>Am. tvaerensis</i>	Pagoda
8.50	0.91	-28.43	0.029	<i>Am. tvaerensis</i>	Pagoda

<sup>a</sup> Measured section begins at the Miaopo Shale/ Pagoda Formation contact.

<sup>b</sup> Fractional weight of total organic carbon in each sample.

sequence, and K-bentonite event stratigraphy the GICE can be correlated from Baltoscandia to North America (e.g., Ainsaar et al., 1999; Saltzman et al., 2003; Kaljo et al., 2007). Additionally, the recognition of the upper part of the *C. bicornis* Graptolite Zone in the Miaopo Shale (An, 1987; Bergström et al., in press), underlying the Pagoda Formation, correlates well with the appearance of this graptolite zone before the GICE in the Fittstown, Oklahoma section (Young et al., 2005), and supports the conodont correlations.

**Table 2**  
Stable Isotope data, Fittstown, Oklahoma

Meters <sup>a</sup>	$\delta^{13}\text{C}_{\text{carb}}$	$\delta^{13}\text{C}_{\text{org}}$	%TOC	Conodont Zone	N. Am. Stage	Formation
0.0	0.06	-28.43	0.024	<i>P. undatus</i>	Turinian	Bromide
5.0	0.02	-26.22	0.071	<i>P. undatus</i>	Turinian	Bromide
8.0	-0.83	-27.70	0.043	<i>P. undatus</i>	Turinian	Bromide
11.0	0.81	-26.90	0.092	<i>P. undatus</i>	Chatfieldian	Viola Springs
13.3	-0.03	-26.44	0.021	<i>P. undatus</i>	Chatfieldian	Viola Springs
14.5	-0.24	-26.65	0.028	<i>P. undatus</i>	Chatfieldian	Viola Springs
16.0	-0.73	-26.66	0.036	<i>P. undatus</i>	Chatfieldian	Viola Springs
17.5	-0.21	-26.87	0.036	<i>P. undatus</i>	Chatfieldian	Viola Springs
19.3	-1.01	-26.33	0.016	<i>P. undatus</i>	Chatfieldian	Viola Springs
20.5	0.19	-26.32	0.009	<i>P. undatus</i>	Chatfieldian	Viola Springs
22.3	-0.40	-26.86	0.010	<i>P. undatus</i>	Chatfieldian	Viola Springs
30.3	-0.18	-26.01	0.004	<i>P. tenuis</i>	Chatfieldian	Viola Springs
31.0	-0.21	-26.24	0.010	<i>P. tenuis</i>	Chatfieldian	Viola Springs
33.0	0.15	-26.55	0.004	<i>P. tenuis</i>	Chatfieldian	Viola Springs
35.0	0.11	-24.73	0.014	<i>P. tenuis</i>	Chatfieldian	Viola Springs
39.0	0.32	-25.57	0.009	<i>P. tenuis</i>	Chatfieldian	Viola Springs
41.0	0.70	-25.95	0.003	<i>P. tenuis</i>	Chatfieldian	Viola Springs
44.0	0.91	-27.84	0.051	<i>P. tenuis</i>	Chatfieldian	Viola Springs
45.0	0.87	-29.12	0.091	<i>P. tenuis</i>	Chatfieldian	Viola Springs
47.0	0.97	-29.52	0.104	<i>P. tenuis</i>	Chatfieldian	Viola Springs
49.0	1.22	-29.14	0.104	<i>P. tenuis</i>	Chatfieldian	Viola Springs
51.0	1.38	-29.95	0.122	<i>P. tenuis</i>	Chatfieldian	Viola Springs
53.0	1.33	-29.93	0.089	<i>P. tenuis</i>	Chatfieldian	Viola Springs
55.0	1.34	-29.57	0.039	<i>P. tenuis</i>	Chatfieldian	Viola Springs
59.0	0.93	-28.96	0.098	<i>P. tenuis</i>	Chatfieldian	Viola Springs
61.0	1.09	-29.93	0.106	<i>P. tenuis</i>	Chatfieldian	Viola Springs
63.0	1.11	-32.15	0.082	<i>P. tenuis</i>	Chatfieldian	Viola Springs
65.0	1.04	-31.69	0.032	<i>P. tenuis</i>	Chatfieldian	Viola Springs
67.0	-0.33	-31.86	0.018	<i>P. tenuis</i>	Chatfieldian	Viola Springs
71.0	-0.62	-31.53	0.019	<i>B. confluens</i>	Chatfieldian	Viola Springs
73.0	0.38	-31.71	0.028	<i>B. confluens</i>	Chatfieldian	Viola Springs

<sup>a</sup> Section begins 10 m below the Viola Springs/Bromide Contact.

### 3. Methods

Samples were collected from all three sections at 25 to 50 cm intervals and previously analyzed for  $\delta^{13}\text{C}_{\text{carb}}$  (Young et al., 2005; Bergström et al., in press). For  $\delta^{13}\text{C}_{\text{org}}$  studies here, 31 samples from the Fittstown section, 48 samples from the Dolly Ridge section, and 21 samples from the Puxihe section were analyzed. Fresh rock surfaces were generated by a water-based diamond-blade saw and the resulting thin-section billets were polished, and placed into an ultrasonic bath containing ultrapure (deionized, 18 M $\Omega$ ) water to remove surficial organic contaminants. Micritic (fine-grained) components were microdrilled (~1.5 g of powder) from the thin-section billets.

Micritic components and bulk carbonate have been previously demonstrated to record original  $\delta^{13}\text{C}_{\text{carb}}$  signatures from Upper Ordovician seas (Gao et al., 1996; Ainsaar et al., 1999; Young et al., 2005; Panchuk et al., 2006; Fanton and Holmden, 2007). This is supported by the following arguments: 1) brachiopod calcite and micrite based  $\delta^{13}\text{C}_{\text{carb}}$  curves yield similar trends and isotopic values (e.g., Bergström et al., 2006; Brenchley et al., 1994, 2003; Long, 1993); 2) modeling studies indicate that  $\delta^{13}\text{C}_{\text{carb}}$  values of marine carbonates

**Table 3**  
Stable Isotope data, Dolly Ridge, West Virginia

Meters <sup>a</sup>	$\delta^{13}\text{C}_{\text{carb}}$	$\delta^{13}\text{C}_{\text{org}}$	%TOC <sup>b</sup>	Conodont Zone	N. Am. Stage	Formation
0.0	1.44	-27.20	0.066	<i>P. undatus</i>	Turinian	Nealmont
2.0	1.49	-26.68	0.053	<i>P. undatus</i>	Turinian	Nealmont
4.0	1.38	-27.30	0.057	<i>P. undatus</i>	Turinian	Nealmont
5.0	1.18	-27.21	0.062	<i>P. undatus</i>	Chatfieldian	Nealmont
5.5	1.19	-27.46	0.047	<i>P. undatus</i>	Chatfieldian	Nealmont
8.1	0.70	-27.48	0.054	<i>P. undatus</i>	Chatfieldian	Nealmont
10.1	1.00	-27.44	0.062	<i>P. undatus</i>	Chatfieldian	Nealmont
12.1	0.96	-27.23	0.052	<i>P. undatus</i>	Chatfieldian	Nealmont
14.1	0.97	-27.64	0.061	<i>P. undatus</i>	Chatfieldian	Nealmont
16.1	0.29	-28.85	0.018	<i>P. undatus</i>	Chatfieldian	Nealmont
18.1	1.07	-27.24	0.056	<i>P. undatus</i>	Chatfieldian	Nealmont
20.1	0.95	-28.07	0.074	<i>P. undatus</i>	Chatfieldian	Nealmont
22.1	0.92	-26.90	0.028	<i>P. undatus</i>	Chatfieldian	Nealmont
28.1	0.36	-27.71	0.032	<i>P. undatus</i>	Chatfieldian	Nealmont
34.1	0.82	-27.77	0.064	<i>P. undatus</i>	Chatfieldian	Nealmont
42.6	0.88	-26.74	0.056	<i>P. undatus</i>	Chatfieldian	Nealmont
44.6	0.44	-26.87	0.076	<i>P. undatus</i>	Chatfieldian	Nealmont
46.6	0.42	-25.93	0.082	<i>P. undatus</i>	Chatfieldian	Nealmont
48.0	0.49	-25.39	0.092	<i>P. undatus</i>	Chatfieldian	Nealmont
49.5	0.57	-26.75	0.022	<i>P. undatus</i>	Chatfieldian	Dolly Ridge
51.5	1.17	-27.32	0.062	<i>P. tenuis?</i>	Chatfieldian	Dolly Ridge
54.5	0.98	-27.38	0.047	<i>P. tenuis?</i>	Chatfieldian	Dolly Ridge
59.5	1.01	-27.85	0.032	<i>P. tenuis?</i>	Chatfieldian	Dolly Ridge
66.5	1.14	-27.23	0.085	<i>P. tenuis</i>	Chatfieldian	Dolly Ridge
71.5	2.05	-27.48	0.105	<i>P. tenuis</i>	Chatfieldian	Dolly Ridge
75.5	2.27	-26.83	0.068	<i>P. tenuis</i>	Chatfieldian	Dolly Ridge
80.5	2.90	-26.85	0.146	<i>P. tenuis</i>	Chatfieldian	Dolly Ridge
87.5	2.75	-26.77	0.149	<i>P. tenuis</i>	Chatfieldian	Dolly Ridge
93.5	3.10	-26.52	0.128	<i>P. tenuis</i>	Chatfieldian	Dolly Ridge
99.5	3.29	-26.74	0.368	<i>P. tenuis</i>	Chatfieldian	Dolly Ridge
106.5	3.09	-26.63	0.107	<i>P. tenuis</i>	Chatfieldian	Dolly Ridge
118.5	2.85	-26.91	0.273	<i>P. tenuis</i>	Chatfieldian	Dolly Ridge
122.5	3.02	-26.28	0.185	<i>P. tenuis</i>	Chatfieldian	Dolly Ridge
129.5	3.00	-26.29	0.213	<i>P. tenuis</i>	Chatfieldian	Dolly Ridge
134.2	2.92	-26.44	0.173	<i>P. tenuis</i>	Chatfieldian	Dolly Ridge
147.2	2.74	-26.75	0.050	<i>P. tenuis</i>	Chatfieldian	Dolly Ridge
152.2	2.37	-26.77	0.113	<i>P. tenuis</i>	Chatfieldian	Dolly Ridge
158.2	2.17	-26.82	0.195	<i>P. tenuis</i>	Chatfieldian	Dolly Ridge
161.2	2.32	-27.24	0.051	<i>P. tenuis</i>	Chatfieldian	Dolly Ridge
163.2	1.39	-26.38	0.133	<i>P. tenuis</i>	Chatfieldian	Dolly Ridge
171.2	1.44	-27.38	0.333	<i>P. tenuis?</i>	Chatfieldian	Dolly Ridge
175.2	0.50	-26.66	0.064	<i>P. tenuis?</i>	Chatfieldian	Dolly Ridge
179.2	0.62	-27.71	0.071	<i>B. confluens?</i>	Chatfieldian	Dolly Ridge
183.2	-0.37	-28.06	0.101	<i>B. confluens?</i>	Chatfieldian	Dolly Ridge
187.2	1.29	-27.66	0.263	<i>B. confluens?</i>	Chatfieldian	Reedsville

<sup>a</sup> Base of section 7 m below first reported N-1 K-bentonite bed of Perry (1972) in the Nealmont Formation.

are largely rock-buffered during diagenesis (e.g., Banner and Hanson, 1990); and 3) many Paleozoic positive  $\delta^{13}\text{C}$  excursions have been documented in a wide variety of lithologies on several paleocontinents (e.g., Saltzman et al., 2000; Saltzman, 2002; Brenchley et al., 2003; among others). Micrite and bulk carbonate may also contain sufficient and well preserved organic matter for  $\delta^{13}\text{C}_{\text{org}}$  analyses (e.g., Patzkowsky et al., 1997; Pancost et al., 1999; Melchin and Holmden, 2006). Although alteration of primary  $\delta^{13}\text{C}_{\text{org}}$  values may occur (e.g., due to thermal alteration or oxidative loss of certain organic compounds; (see section 5.1 for a complete discussion of factors affecting  $\delta^{13}\text{C}_{\text{org}}$ ) and may be more difficult to recognize than for  $\delta^{13}\text{C}_{\text{carb}}$ , we observe no systematic relationship between  $\delta^{13}\text{C}_{\text{org}}$  and wt.% TOC (see Tables 1–3) that might be expected if differential alteration of organic matter occurred in horizons that are poor versus those which are relatively rich in organic carbon.

Sample powders were accurately weighed and acidified using 6N HCl to remove carbonate minerals. Insoluble fractions were then repeatedly rinsed in ultrapure water and dried at 85 °C. Remaining residues were weighed and homogenized, and then loaded into tin capsules. Samples were combusted with a Costech Elemental Analyzer

and the resulting  $\text{CO}_2$  gas analyzed for  $\delta^{13}\text{C}$  through a Finnigan Delta IV stable isotope ratio mass spectrometer under continuous flow using an open-split CONFLO III interface in the Stable Isotope Biogeochemistry Laboratory at the Ohio State University. Carbon isotope ratios presented here are reported in per mil notation relative to the Vienna Pee Dee Belmenite limestone standard (‰ VPDB). Repeated measurements of the IAEA-CH7 standards were  $\pm 0.15\text{‰}$  for  $\delta^{13}\text{C}$ , and  $\pm 1.0\text{‰}$  for  $\text{‰C}$  (1 standard deviation). Weight percent of total organic carbon (TOC) in samples is determined by comparison of voltages for the ion beam intensities of masses 44, 45, and 46  $\text{CO}_2^+$  between our samples and known wt.% carbon of the gravimetric standard Acetanilide.

## 4. Results

### 4.1. Puxihe, Hubei Province, southeastern China

A complete section of the Pagoda Formation is exposed in the Puxihe Quarry, north of Yichang City in Hubei Province, China (Fig. 2). Values of  $\delta^{13}\text{C}_{\text{carb}}$  begin at +0.7‰ in the lowermost beds of the Pagoda Formation and abruptly trend to +2.4‰ near the first appearance of

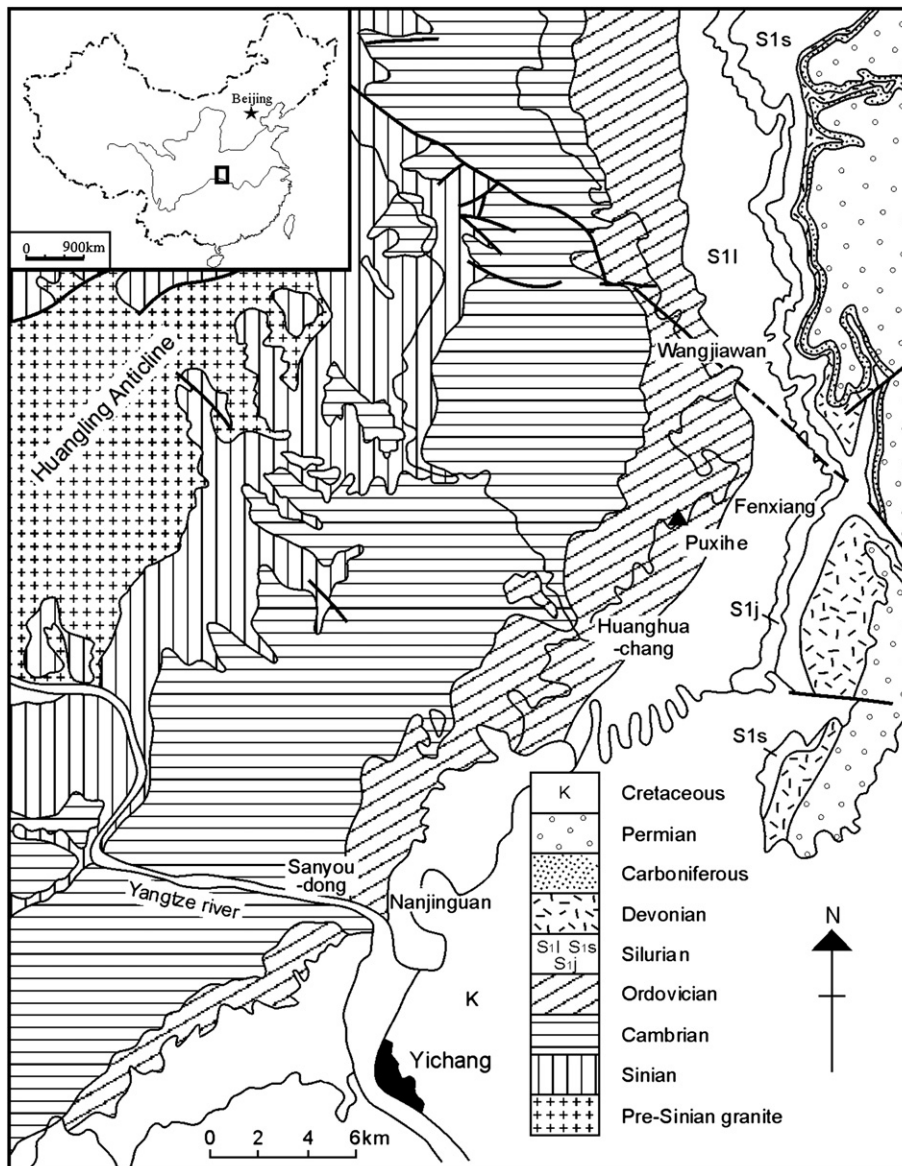


Fig. 2. Geologic Map of south-central China, near Yichang City in Hubei Province. Marked on this map is the Puxihe Quarry sample locality (triangle), northeast of Yichang City.

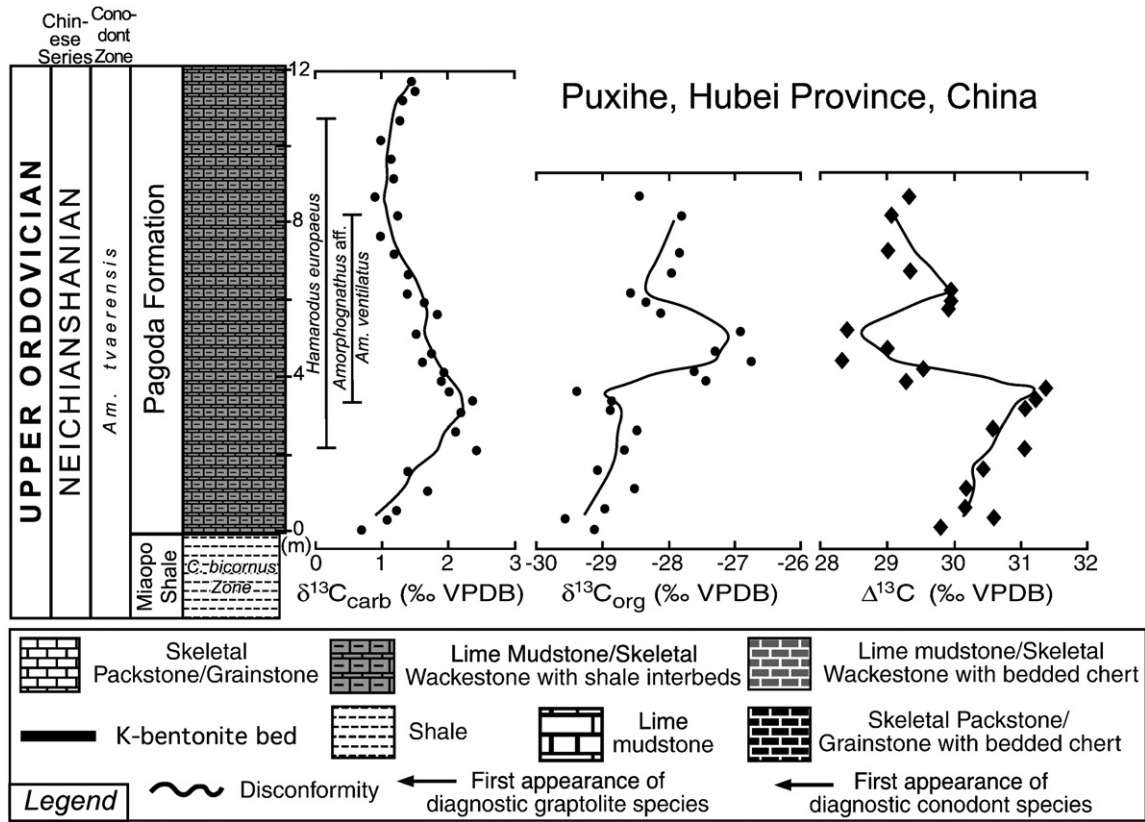


Fig. 3. Paired carbon isotope data from the Puxihe Quarry (Hubei Province), China, with diagnostic conodonts and graptolite ranges plotted for the Pagoda and Miaopo Shale Formations (biostratigraphy from An, 1987; Chen et al., 1995; Bergström et al., in press). Three point running average curves are fitted to the data, note the positive  $\delta^{13}C_{org}$  excursion occurs in the declining limb of the  $\delta^{13}C_{carb}$  curve, and coincident abrupt drop in  $\Delta^{13}C$  values. Note that  $\Delta^{13}C = \delta^{13}C_{carb} - \delta^{13}C_{org}$ .

the diagnostic conodont *H. europaeus* (Bergström et al., in press).  $\delta^{13}C_{org}$  values begin near  $-29.5\text{‰}$  and trend positively towards  $-28.5\text{‰}$  (Fig. 3). As  $\delta^{13}C_{carb}$  values begin to decline at 3.5 m,  $\delta^{13}C_{org}$  values shift abruptly positive reaching a peak value of  $-26.7\text{‰}$  at 4.25 m, above the first appearance of the diagnostic conodont *Amorphognathus* aff. *Am. ventulatus* in the middle of the Pagoda Formation.  $\delta^{13}C_{org}$  values shift back to  $-28.1\text{‰}$  at 5.5 m and stay near this value while at the same time  $\delta^{13}C_{carb}$  values return to base-line values of  $+1.0\text{‰}$  in the upper part of the Pagoda Formation.

$\delta^{13}C_{carb}$  values peak (from 2 to 3.5 m;  $+1.7\text{‰}$  shift) prior to  $\delta^{13}C_{org}$  values (peak values at 3.75 to 5 m;  $+2.8\text{‰}$  shift). The resultant  $\Delta^{13}C$  increases to  $31.4\text{‰}$  initially, but then declines at 4.0 m returning to values of  $28.4\text{‰}$  in the later part of the  $\delta^{13}C_{carb}$  excursion.

4.2. Fittstown, Arbuckle Mountains, southern Oklahoma

The Fittstown section was sampled along Highway 99 in Pontotoc County, Oklahoma (Fig. 4) beginning approximately 10 m below the Bromide/Viola Springs Formation contact.  $\delta^{13}C_{carb}$  values begin between  $-1.0\text{‰}$  and  $0.0\text{‰}$  (Fig. 5) in the upper Bromide Formation (*P. undatus* Zone), while  $\delta^{13}C_{org}$  values start out at  $-28.4\text{‰}$  and rise slightly to a value of  $-27.7\text{‰}$  near contact with the Viola Springs Formation. Above, in the first  $\sim 10$  m of cherty lime mudstone-wackestone facies of the Viola Springs Formation (upper part of the *P. undatus* and *C. bicornis* conodont and graptolite zones, respectively)  $\delta^{13}C_{carb}$  values stay between  $-1.0\text{‰}$  and  $0.0\text{‰}$ , and  $\delta^{13}C_{org}$  values shift heavier to  $-26.5\text{‰}$ . In the overlying 20 m of cherty packstone facies both  $\delta^{13}C_{carb}$  and  $\delta^{13}C_{org}$  values trend heavier, in the *P. tenuis* Zone.  $\delta^{13}C_{org}$  reaches a peak of  $-24.7\text{‰}$  at 35 m and then rapidly falls to  $-29.1\text{‰}$  in the next 10 m of the section.  $\delta^{13}C_{carb}$  values continue to rise to  $+1.5\text{‰}$  in the overlying non-cherty packstone/grainstone facies, while  $\delta^{13}C_{org}$  values decline to values near  $-29.5\text{‰}$ . In the lime

mudstone/wackestone facies near the top of the section (*B. confluens* Zone)  $\delta^{13}C_{org}$  values shift even lighter to values averaging  $-31.5\text{‰}$ .

The general trend of  $\delta^{13}C_{org}$  is to heavier values in the lower Viola Springs Formation, then to lighter values near the disappearance of

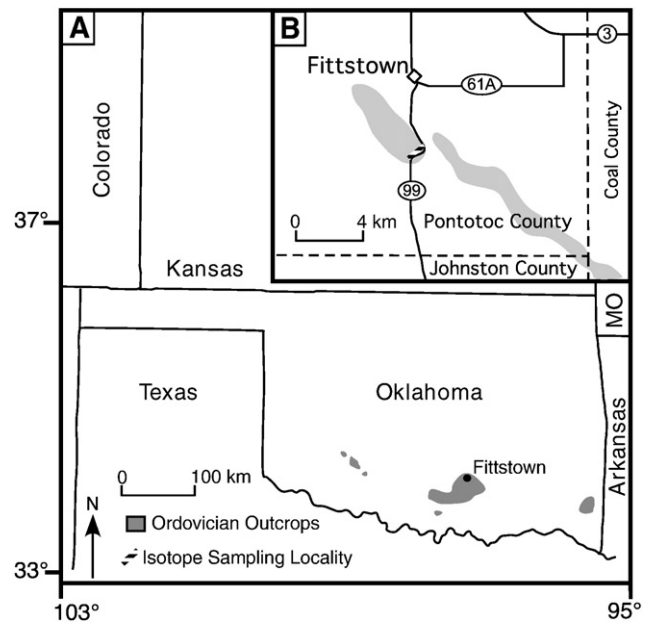
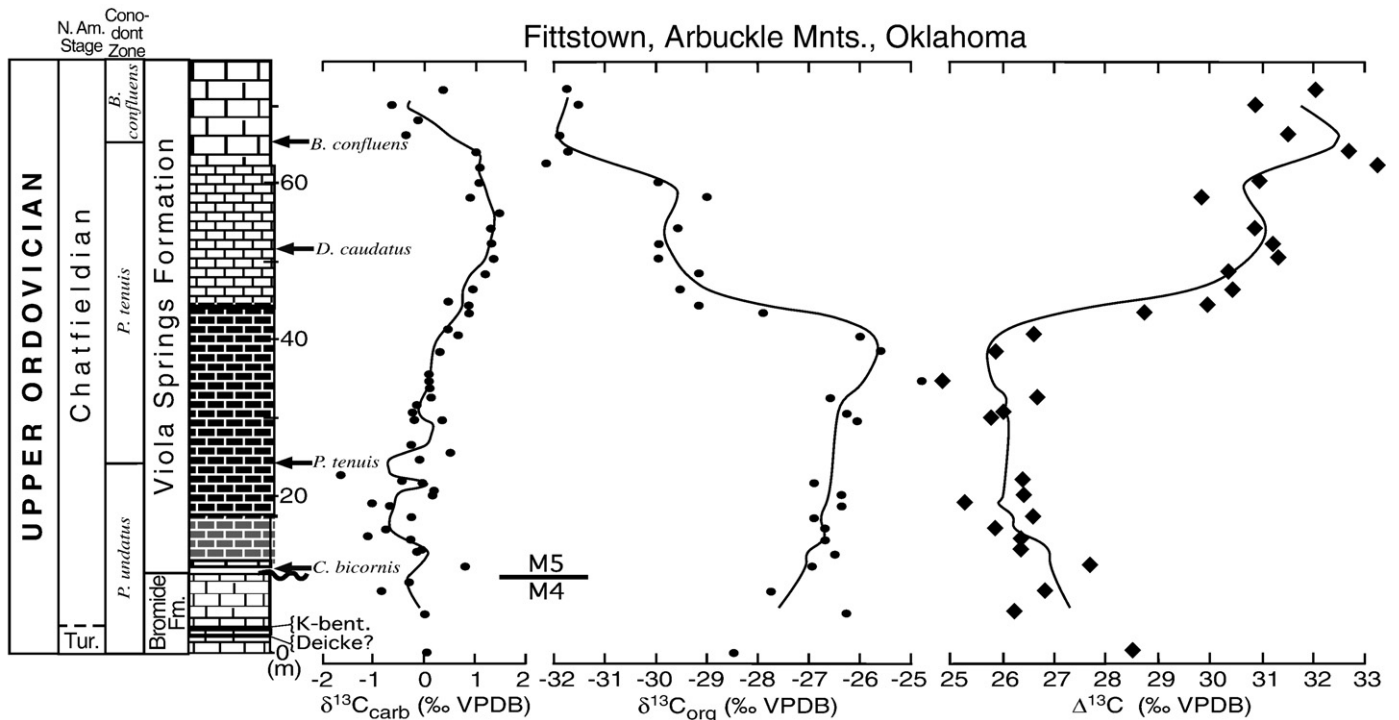


Fig. 4. A, Map of south-central North America showing state outlines and Ordovician outcrops in Oklahoma (OK). B, Inset map showing the location of the roadcut along Highway 99, south of Fittstown (grey area, outcrops of the Viola Springs Formation) (after Alberstadt, 1973).



**Fig. 5.** Paired carbon isotope data from the Fittstown section, Arbuckle Mountains, Oklahoma. Also plotted are important Midcontinent conodont fauna first occurrences from Sweet (1983) and important graptolite occurrences from Finney (1986) and Goldman et al. (2007). Note that the *D. caudatus* Graptolite Biozone is inferred (from conodont, graptolite, chitinozoan, and  $\delta^{13}\text{C}$  data from the nearby GSSP section) to begin within the chert-rich carbonates below the  $\delta^{13}\text{C}_{\text{carb}}$  that are barren of graptolites (Goldman et al., 2007). Three point running average curves are fitted to the data, note the negative  $\delta^{13}\text{C}_{\text{org}}$  excursion coinciding with disappearance of the chert-rich carbonate facies and the positive  $\delta^{13}\text{C}_{\text{carb}}$  excursion.

bedded/nodular chert facies.  $\delta^{13}\text{C}_{\text{org}}$  become lightest at the packstone/grainstone to wackestone/mudstone facies transition. Peak  $\delta^{13}\text{C}_{\text{org}}$  values (from 35 to 41 ms; +6‰ shift) occur prior to peak  $\delta^{13}\text{C}_{\text{carb}}$  values (from 49 to 57 m; +2‰ shift). The resulting isotopic difference ( $\Delta$ ) remains low prior to the  $\delta^{13}\text{C}_{\text{carb}}$  excursion (minimum of ~25‰) and increases through the excursion (maximum of ~33‰).

4.3. Dolly Ridge, Central Appalachians, West Virginia

The Nealmont and Dolly Ridge Formations in Germany Valley were sampled from an outcrop along a farm road in Pendleton County, West Virginia, near the town of Riverton (Fig. 6). Lime mudstones of the lower Nealmont Formation that lie below a 0.4 m thick K-bentonite

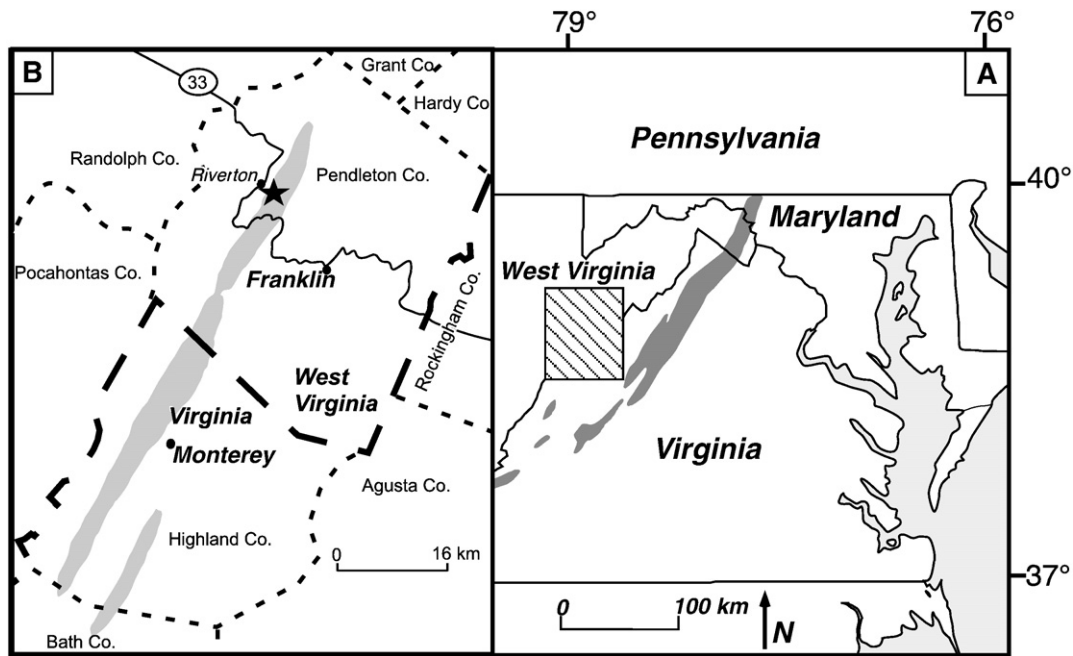


**Fig. 6.** A, Map of eastern North America showing Ordovician outcrops in the central Appalachian Basin Region with state outlines. B, Inset map showing the location of the type-section for the Dolly Ridge Formation (Perry, 1972) outcropping along a farm road just east of Riverton, West Virginia (grey area, outcrops of Dolly Ridge and Reedsville Formations) (after Keith, 1989).

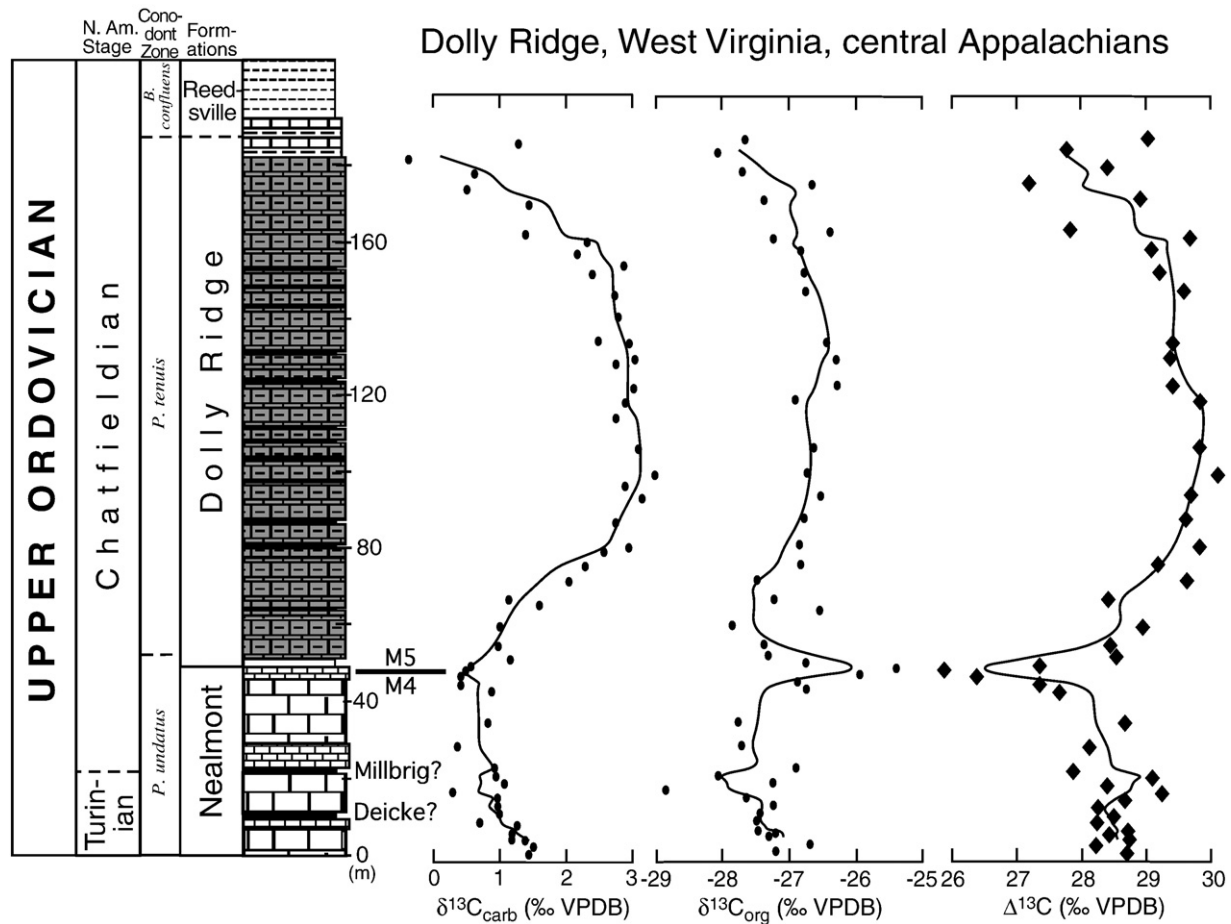


Fig. 7. Paired carbon isotope data from the Dolly Ridge section, central Appalachians, West Virginia. Due to the limited biostratigraphic work within the Dolly Ridge Formation (Keith, 1989; Young et al., 2005) a detailed conodont biostratigraphy is not yet possible for this section, however the previous K-bentonite and  $\delta^{13}\text{C}_{\text{carb}}$  work (Perry, 1972; Young et al., 2005) allow us to tie into nearby sections with more detailed biostratigraphy. Three point running average curves are fitted to the data, note that  $\Delta^{13}\text{C}$  tracks the  $\delta^{13}\text{C}_{\text{carb}}$  curve, with a conspicuous short-lived positive  $\delta^{13}\text{C}_{\text{org}}$  excursion at top of the Nealmont Formation.

bed, within the *P. undatus* Zone, record  $\delta^{13}\text{C}_{\text{carb}}$  values from +1.5 to +1.0‰ and stay between 0.0‰ and +0.9‰ through the crinoidal packstones at the top of the Nealmont Formation (Fig. 7).  $\delta^{13}\text{C}_{\text{org}}$  values fluctuate between -27.2‰ and -28.0‰ with a curious shift to -25.4‰ in two samples from the uppermost few meters of the Nealmont. Across the Nealmont/Dolly Ridge Formation contact  $\delta^{13}\text{C}_{\text{org}}$  values decline to -27.8‰, while  $\delta^{13}\text{C}_{\text{carb}}$  values begin to shift positively +1.0‰ in the deeper water interbedded dark lime mudstone/shale facies. As  $\delta^{13}\text{C}_{\text{carb}}$  values continue to rise in the Dolly Ridge Formation, maximum values of +3.3‰ to +2.7‰ are reached between 87 and 155 m, within the *P. tenuis* Zone. In this same interval  $\delta^{13}\text{C}_{\text{org}}$  values also rise to a peak of -26.3‰. Approaching the gradational Dolly Ridge/Reedsville Formation contact and the *P. tenuis*/*B. confluens* zonal boundary (Keith, 1989),  $\delta^{13}\text{C}_{\text{carb}}$  and  $\delta^{13}\text{C}_{\text{org}}$  values decline again to near 0.0‰ and -28.0‰, respectively.

During the  $\delta^{13}\text{C}_{\text{carb}}$  excursion of magnitude  $\sim +2.5$ ‰ in the Dolly Ridge Formation,  $\delta^{13}\text{C}_{\text{org}}$  appears to generally track  $\delta^{13}\text{C}_{\text{carb}}$  values, with the exception of the brief +3‰  $\delta^{13}\text{C}_{\text{org}}$  shift in the uppermost Nealmont Formation.  $\Delta^{13}\text{C}$  decreases in the uppermost Nealmont and then increases in the overlying Dolly Ridge Formation, but then  $\Delta^{13}\text{C}$  decreases again in the upper Dolly Ridge Formation.

## 5. Discussion

The three well correlated, late Sandbian to early Katian successions presented here record different  $\delta^{13}\text{C}_{\text{org}}$  trends (Fig. 8), despite all sections recording a global positive  $\delta^{13}\text{C}_{\text{carb}}$  excursion (GICE). While

trends in  $\delta^{13}\text{C}_{\text{org}}$  and the resulting  $\Delta^{13}\text{C}$  curve recorded from south China are similar to previously documented trends from Iowa and Pennsylvania (Patzkowsky et al., 1997; Pancost et al., 1999), trends from West Virginia and Oklahoma are markedly different. Here we first evaluate factors that may affect  $\delta^{13}\text{C}_{\text{carb}}$  and  $\delta^{13}\text{C}_{\text{org}}$  values to produce stratigraphic trends in  $\Delta^{13}\text{C}$  (e.g., Hayes et al., 1999). We then interpret each individual stratigraphic  $\Delta^{13}\text{C}$  ( $\Delta^{13}\text{C} = \delta^{13}\text{C}_{\text{carb}} - \delta^{13}\text{C}_{\text{org}}$ ) trend in the context of global changes in  $p\text{CO}_2$  predicted by models as well as local water mass characteristics (i.e., 'aquafacies') observed in previous studies (e.g., Holmden et al., 1998; Young et al., 2005; Panchuk et al., 2006).

### 5.1. Factors affecting the isotopic difference between $\delta^{13}\text{C}_{\text{carb}}$ and $\delta^{13}\text{C}_{\text{org}}$

Several processes contribute to the isotopic difference between  $\delta^{13}\text{C}_{\text{carb}}$  and  $\delta^{13}\text{C}_{\text{org}}$  ( $\Delta^{13}\text{C}$ ), including: 1) the temperature dependent fractionation between dissolved inorganic carbon (DIC) and  $\text{CO}_2(\text{aq})$  in seawater, and the fractionation between DIC and precipitated carbonate minerals (e.g., calcite versus aragonite), 2) photosynthetic fractionation ( $\epsilon_p$ ) associated with carbon fixation by primary producers, and 3) organic matter source variation, secondary biological fractionation (i.e., heterotrophy) and/or diagenesis (e.g., due to thermal maturation) (Hayes et al., 1999; Kienast et al., 2001; Royer et al., 2001).

The large isotopic enrichment ( $\sim +8$ ‰ to  $+12$ ‰) that takes place when  $\text{CO}_2(\text{aq})$  equilibrates with DIC is temperature dependent ( $0.12$ ‰/°C) (Goericke and Fry, 1994). This produces differences

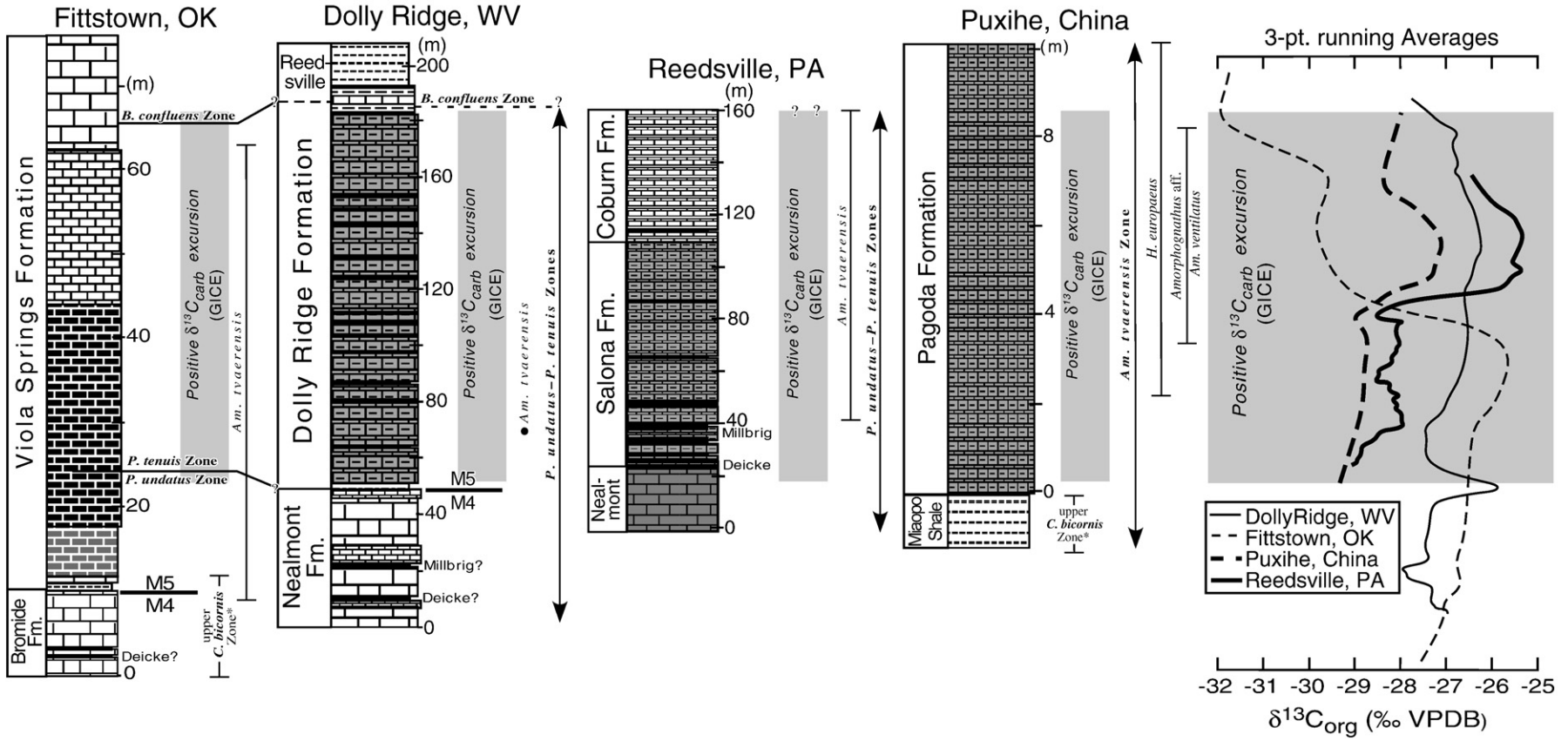


**Fig. 8.** Correlation of the three sections studied here to the previously studied Reedsville, Pennsylvania section (Patzkowsky et al., 1997) and comparison of  $\delta^{13}\text{C}_{\text{org}}$  three-point running average curves from all four sections. This correlation utilizes all previously studied biostratigraphy, sequence stratigraphy, and K-bentonite event stratigraphy (see text for respective references). Note that the grey rectangle indicates where  $\delta^{13}\text{C}_{\text{carb}}$  values deviate positively from a baseline and later return to baseline values (GICE) in all sections. Also note the varying scales of the sections, indicating that apparent net rock accumulation rates during the GICE were quite different between these sections (e.g., Leslie and Bergström, 1997). Thus,  $\delta^{13}\text{C}_{\text{org}}$  three-point running average curves from all sections were scaled respectively to conform to the defined area (grey rectangle) of the GICE defined and shown here.

between water masses at high versus low latitudes (Rau et al., 1989) and can also be significant on long geological timescales (Hayes et al., 1999). For example, global cooling from the Oligocene to Pleistocene has been suggested to account for ~1‰ of an 8‰ decline in observed  $\Delta^{13}\text{C}$  values over this time period (Hayes et al., 1999). In contrast, the isotopic enrichment that occurs when DIC is converted to sedimentary carbonate is relatively small (calcite or aragonite, ~+1‰ and +2.5‰, respectively) by comparison, and not significantly correlated with temperature (Romanek et al., 1992).

As with the majority of carbonates forming today, the Katian sections discussed here were deposited in relatively shallow tropical-subtropical settings, and likely experienced only minor fluctuations in temperatures. For example, tropical seas only varied by 1–2 °C during the last glacial-interglacial transition in the late Quaternary (CLIMAP, 1981). Although sea surface temperatures are expected to drop in the later part of the GICE due to lowered atmospheric  $p\text{CO}_2$  levels (e.g., Patzkowsky et al., 1997), only minor temperature changes are expected for these Katian carbonates deposited between 5°S and 20°S paleolatitude (see Fig. 1). This is supported by relatively small changes in sea surface temperatures (~24–26 °C) that were recently calculated using conodont  $\delta^{18}\text{O}$  data through the Viola Springs Formation at the Fittstown, Oklahoma section (Rosenau et al., 2007). These temperature fluctuations would only account for ~0.25‰ of the 3 to 5‰ shifts in  $\Delta^{13}\text{C}$  values seen in the various sections described here (Fig. 9). Furthermore, there is no evidence for distinct mineralogic differences (i.e., calcite to dolomite) during the GICE interval in the sections studied here that would have contributed significantly to the observed shifts in  $\Delta^{13}\text{C}$ .

The carbon isotope fractionation associated with photosynthetic production ( $\epsilon_p$ ) of organic matter is dependent on many factors, including cell growth rates and  $[\text{CO}_{2(\text{aq})}]$ , that likely varied through the Katian and also between individual sections studied here. Unlike the inorganic isotope fractionation effects discussed above,  $\epsilon_p$  can be large ranging from 8 to 18‰ in the modern oceans (e.g., Francois et al., 1993; Bidigare et al., 1997). Before proceeding with discussion of these primary biological factors (see section 5.2 below), we first present our case for why secondary and source effects are unlikely to play a dominant role in the patterns we observed.

The sedimentary total organic carbon (TOC) analyzed from our sections is expected to be largely from marine sources during the



**Fig. 9.** Comparison of  $\Delta^{13}\text{C}$  three-point running average curves from Oklahoma, south China, and the previously studied Pennsylvania section (Patzkowsky et al., 1997).  $\Delta^{13}\text{C}$  three-point running average curves from these sections have been scaled respectively to conform the area of the GICE (grey rectangle) as defined in Fig. 8. Note that the Oklahoma  $\Delta^{13}\text{C}$  curve is entirely opposite the south China and Pennsylvania trends.

Ordovician time period that significantly predates the earliest land plant megafossils in the Silurian (e.g., Steemans and Wellman, 2004). Although microfossils (cryptospores) of purported terrestrial origin (bryophyte-like plants) have been documented in Middle Ordovician marine rocks (Strother et al., 1996), the earliest report of cryptospores in eastern North America is from younger Hirnantian strata (Richardson and Ausich, 2007). Additionally this terrestrial source is not expected to significantly vary in the  $\delta^{13}\text{C}$  of TOC, as extant Devonian bryophytes have an average  $\delta^{13}\text{C}$  value of -29.4‰ (Jahren et al., 2003), which is well within the range of compound-specific isotopic values of purported Ordovician photoautotrophic sources (Pancost et al., 1999).

Although contributions from terrestrial sources are not expected, heterotrophic organisms likely make up some percent of the TOC reported here. The secondary biological process of respiratory remineralization of organic matter in sediments deposited under oxic conditions has been shown to shift  $\delta^{13}\text{C}_{\text{org}}$  values positively by  $\leq +1.5\%$  (Hayes et al., 1989; Gong and Hollander, 1997; Fischer et al., 1998). Further enrichment of up to +3‰ has been documented in sediments underlying oxygen-depleted waters (Laarkamp and Raymo, 1995; Fischer et al., 1998). The carbonates in our studied sections were mostly deposited under relatively well-oxygenated conditions in shallow epeiric sea settings, although the lowermost ~10 m of the Viola Springs Formation at the Fittstown section may have been deposited under dysoxic conditions. However, in the absence of data from compound-specific studies needed to demonstrate the importance of secondary biological products in our sections, we assume that offsets between primary and secondary producers in our analyzed organic matter were relatively small ( $\leq +1.5\%$ ) and constant (Hayes et al., 1999). Although this assumption is consistent with a study of Late Devonian sediments (deposited under poorly oxygenated waters) that revealed nearly identical trends in  $\delta^{13}\text{C}$  of TOC compared to compound-specific  $\delta^{13}\text{C}_{\text{org}}$  analyses derived from primary producers (i.e., short chain *n*-alkanes, pristane, phytane) (Joachimski et al., 2002), it may not be the case here.

In addition to organic matter source and secondary biological effects, diagenetic factors can also affect  $\delta^{13}\text{C}$  of TOC. Mobilization of isotopically light organic compounds via thermal maturation can shift the  $\delta^{13}\text{C}_{\text{org}}$  values of sedimentary TOC positively by as much as 2‰ (Clayton, 1991; Hayes et al., 1999). An indicator of thermal history is provided by color alteration of conodonts from our study sections that have been assigned conodont alteration index (CAI) values of 1.5, 4.5, and 2 for Oklahoma, West Virginia, and south China, respectively. The CAI values indicate that Oklahoma and south China experienced burial temperatures  $\leq 100$  °C, while the West Virginia section is classified as mature to supermature experiencing burial temperatures  $> 100$  °C (cf. Epstein et al., 1977; Sweet, 1983; An, 1987; Nowlan and Barnes, 1987; Keith, 1989). Thermal history differences could partly explain offsets in  $\delta^{13}\text{C}_{\text{org}}$  values between various sections (see Fig. 8), but would be an unlikely explanation for the differing stratigraphic trends in  $\delta^{13}\text{C}_{\text{org}}$  and  $\Delta^{13}\text{C}$  because a uniform thermal effect across an entire outcrop is expected.

## 5.2. Photosynthetic fractionation $\epsilon_p$ and its influence on $\delta^{13}\text{C}$ trends through the GICE

Although the above discussions make clear that compound-specific isotope work could provide important variations on  $\Delta^{13}\text{C}$  trends described here, we assume that the dominant control on the overall trends in  $\Delta^{13}\text{C}$  observed in different sections were changes in factors that influence the magnitude of primary photosynthetic fractionation of  $^{12}\text{C}$  ( $\epsilon_p$ ) including  $[\text{CO}_{2(\text{aq})}]$  and growth rate. Laboratory and field studies of modern marine phytoplankton have shown that  $\epsilon_p$  decreases as growth rates increase, as the ratio of cell volume to surface area (*V/S*) increases, or as  $\text{CO}_{2(\text{aq})}$  concentrations decrease (see Fig. 10; Freeman and Hayes, 1992; Francois et al., 1993; Laws et al., 1995; Bidigare et al., 1997; Popp et al., 1998; Hayes et al.,

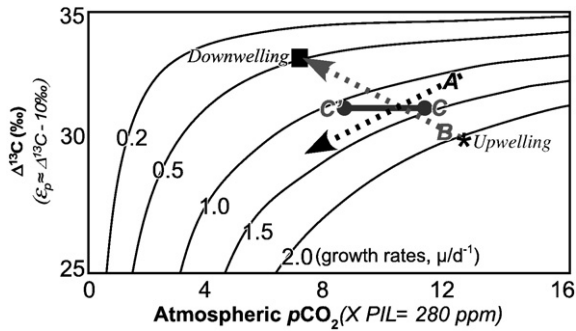


**Fig. 10.** Generalized relationship between the photosynthetic fractionation effect ( $\epsilon_p$ ), atmospheric  $\text{CO}_2$  levels, and modern marine phytoplankton growth rates ( $\mu/\text{day}$ ) assuming a constant volume/surface ratio of  $1\mu\text{m}$  (modified from Hayes et al., 1999; Joachimski et al., 2002). Note that pre-industrial levels (PIL) of atmospheric  $p\text{CO}_2$  (280 ppm) were used here (e.g., Herrmann et al., 2003, 2004). The large isotopic difference between  $\delta^{13}\text{C}_{\text{carb}}$  and  $\delta^{13}\text{C}_{\text{org}}$  ( $\Delta^{13}\text{C}$ ) is mainly due to  $\epsilon_p$  (e.g., Hayes et al., 1999). Track A (black-dashed arrow) would be indicative of areas in which marine primary producers maintained consistent growth rates and  $\epsilon_p$  was dominantly influenced by a lowering of  $\text{CO}_{2(\text{aq})}$  concentrations in seawater (Pennsylvania, Iowa, south China). Track B (grey-dashed arrow) would be indicative of areas where declining growth rates of primary producers were greatly influencing  $\epsilon_p$ , masking a relative lowering of atmospheric  $p\text{CO}_2$  levels (i.e.,  $\Delta^{13}\text{C}$  increasing in Oklahoma). Track C-C' (time slices in Fig. 11) demonstrates how a relative lowering of growth rates of primary producers can overprint a lowering of atmospheric  $p\text{CO}_2$  levels, resulting in steady  $\Delta^{13}\text{C}$  values of West Virginia during the GICE. See text for discussion of upwelling and downwelling waters on growth rates and  $\epsilon_p$ .

1999). We first discuss the interpretation of the previously investigated Pennsylvania  $\Delta^{13}\text{C}$  trend of Patzkowsky et al. (1997) and use this as a reference section for comparison among our studied sections.

#### 5.2.1. $\epsilon_p$ in the Pennsylvania reference section

Patzkowsky et al. (1997) showed that  $\delta^{13}\text{C}_{\text{carb}}$  and  $\delta^{13}\text{C}_{\text{org}}$  values initially track one another during the beginning of the GICE. Peak  $\delta^{13}\text{C}_{\text{org}}$  values occur after peak  $\delta^{13}\text{C}_{\text{carb}}$  values, resulting in an abrupt fall in  $\Delta^{13}\text{C}$  in the latter part of the GICE (Fig. 9). Patzkowsky et al. (1997) noted the lack of independent indicators of productivity changes (i.e., chert or phosphate deposits; Pope and Steffen, 2003) and the lack of organic matter source variations (i.e., *Gleocapsomorpha prisca*, an anomalous organic-walled microfossil; Hatch et al., 1987) that could have produced the large changes in  $\delta^{13}\text{C}_{\text{org}}$  from the analyzed carbonates of the Salona and Coburn Formations. Although compound-specific studies of  $\delta^{13}\text{C}_{\text{org}}$  in Iowa through the GICE interval indicated that compounds from *G. prisca* produced relatively heavy sedimentary  $\delta^{13}\text{C}_{\text{org}}$  of TOC in Iowa relative to Pennsylvania (Pancost et al., 1999), this was apparently a localized bloom, as *G. prisca* has not been reported from other sections outside of this region that also document the GICE (Hatch et al., 1987; Fanton and Holmden, 2007). Instead the  $\Delta^{13}\text{C}$  trends from Pennsylvania were interpreted to reflect fluctuations in  $\text{CO}_{2(\text{aq})}$  concentrations (track A in Fig. 10). This interpretation is also consistent with the predicted changes in  $p\text{CO}_2$  during the period of enhanced organic carbon burial suggested by the positive  $\delta^{13}\text{C}_{\text{carb}}$  excursion (GICE), although the precise location of such organic-rich deposits remains poorly known.

The relatively invariant  $\Delta^{13}\text{C}$  trend during rising  $\delta^{13}\text{C}_{\text{carb}}$  in the lower part of the Pennsylvania section was interpreted to reflect high  $p\text{CO}_2$  levels that lie above the sensitivity of marine phytoplankton ( $\sim 12\text{--}15\times\text{PAL}$ ). Carbon dioxide levels continued to fall due to enhanced organic carbon burial and by the later part of the  $\delta^{13}\text{C}_{\text{carb}}$  excursion was in the range of sensitivity of phytoplankton, causing  $\delta^{13}\text{C}_{\text{org}}$  to abruptly increase and shift  $\Delta^{13}\text{C}$  to lower values (Patzkowsky et al., 1997). A cooling event associated with the GICE, consistent with the proposed drop in  $p\text{CO}_2$ , is supported by changes in carbonate deposition style, regional extinction of brachiopods, and modeling studies, all of which suggest climatic cooling associated with

the GICE (Patzkowsky and Holland, 1993; Holland and Patzkowsky, 1996; Pope and Read, 1998; Kump and Arthur, 1999). Additionally, a  $+2\text{--}2.5\%$  shift in  $\delta^{18}\text{O}$  documented in well-preserved brachiopod and marine calcite cements that record the GICE in  $\delta^{13}\text{C}_{\text{carb}}$  from the paleocontinent of Baltica have been attributed to a decrease in seawater temperatures and an increase in salinity during the GICE (Marshall and Middleton, 1990; Tobin et al., 2005).

#### 5.2.2. South China

The overall trend in  $\Delta^{13}\text{C}$  from the paleocontinent of South China is very similar to the Pennsylvania  $\Delta^{13}\text{C}$  trend (Figs. 8 and 9), with peak  $\delta^{13}\text{C}_{\text{org}}$  values occurring later than peak  $\delta^{13}\text{C}_{\text{carb}}$  values. Observed  $\Delta^{13}\text{C}$  trends initially increase (Fig. 9) in the beginning of the GICE and then abruptly fall in the middle of the  $\delta^{13}\text{C}_{\text{carb}}$  excursion. Like Pennsylvania, there are no independent indicators of nutrient or productivity changes through the interbedded shales and lime mudstones of the Pagoda Formation at the Puxihe section. Therefore a decrease in the concentration of  $\text{CO}_{2(\text{aq})}$  (track A in Fig. 10) is a more plausible interpretation, and may provide the first confirmation that the GICE organic matter burial event resulted in a global lowering of  $p\text{CO}_2$ . Although, many other sections of the Pagoda Formation do contain enigmatic sedimentary features (i.e., polygonal cracks) throughout the formation but their origin remains controversial (e.g., Bergström et al., in press) and possible impacts on the type of organic matter preserved are unclear.

#### 5.2.3. Oklahoma

The trend in  $\Delta^{13}\text{C}$  from Oklahoma is entirely opposite to those from Pennsylvania and South China during the GICE (Fig. 9). The  $\Delta^{13}\text{C}$  trend in Oklahoma is driven by the large changes  $\delta^{13}\text{C}_{\text{org}}$  values through the section compared to the relatively small change in  $\delta^{13}\text{C}_{\text{carb}}$  values compared with other sections studied. These  $\delta^{13}\text{C}_{\text{carb}}$  and  $\delta^{13}\text{C}_{\text{org}}$  trends differ from what appears to be the global pattern, possibly due to local changes in phytoplankton growth rates (track B in Fig. 10). This is consistent with the lithologic evidence of bedded cherts and phosphates in Oklahoma that indicate changes in the strength of upwelling along the southern Laurentian margin (Pope, 2004; Young



**Fig. 11.** Comparison of  $\Delta^{13}\text{C}$  three-point running average curves from West Virginia, south China, and the previously studied Pennsylvania section (Patzkowsky et al., 1997). Refer to Figs. 8 and 9 for explanation of scaling of three-point average curves. Note that the south China and Pennsylvania  $\Delta^{13}\text{C}$  curves have very similar trends. West Virginia  $\Delta^{13}\text{C}$  values are initially lower than Pennsylvania and south China (dashed line C), but then later during the GICE  $\Delta^{13}\text{C}$  values become higher (dashed line C'). Refer to Fig. 10 and text for further explanation.

et al., 2005). Bedded cherts and phosphate in the lower part of the section indicate upwelling of nutrient rich waters, and the associated high growth rates may explain the unusually heavy  $\delta^{13}\text{C}_{\text{org}}$  values (and low  $\Delta^{13}\text{C}$ ). Bedded cherts and phosphate disappear upsection, and lowered growth rates may have driven the  $\Delta^{13}\text{C}$  values to increase significantly above this level (Fig. 5).

The explanation of productivity-driven changes in  $\delta^{13}\text{C}_{\text{org}}$  in Oklahoma is consistent with observations in modern upwelling zones. In the modern Peru Upwelling Zone, the correlation of high nutrient ( $\text{PO}_4^{3-}$ ) concentrations and low  $\epsilon_p$  values (heavy  $\delta^{13}\text{C}_{\text{org}}$  values) has been linked to high phytoplankton growth rates (Bidigare et al., 1997). Because of these large swings in phytoplankton growth rates in upwelling zones, late Cenozoic investigations that have examined the use of  $\delta^{13}\text{C}_{\text{org}}$  as a proxy for global changes in  $p\text{CO}_2$  have focused on oligotrophic waters (e.g., Pagani et al., 1999).

#### 5.2.4. West Virginia

The  $\delta^{13}\text{C}_{\text{org}}$  and  $\Delta^{13}\text{C}$  records from Dolly Ridge, West Virginia are somewhat puzzling because they do not more closely reflect the trends observed by Patzkowsky et al. (1997) only ~350 km away in Pennsylvania (Fig. 11). The Pennsylvania and West Virginia sections record similar  $\delta^{13}\text{C}_{\text{carb}}$  values, lithofacies, and conodont biofacies reflecting the same water mass ('aquafacies'; Holmden et al., 1998). However, despite these similarities, the contrasting  $\delta^{13}\text{C}_{\text{org}}$  and  $\Delta^{13}\text{C}$  records between Pennsylvania and West Virginia suggest that the water mass in West Virginia was influenced by an additional factor that is likely to have been local changes in nutrient cycling that influenced phytoplankton growth rates.

It is important to note that, in contrast to the Oklahoma section, the  $\Delta^{13}\text{C}$  trends in the West Virginia section are largely driven by a relatively invariant  $\delta^{13}\text{C}_{\text{org}}$  profile compared to a distinctly trending  $\delta^{13}\text{C}_{\text{carb}}$  profile. These differences in  $\delta^{13}\text{C}_{\text{carb}}$  and  $\delta^{13}\text{C}_{\text{org}}$  profiles could suggest that the West Virginia water mass may represent a zone of mixing between nearby water masses over Laurentia (Southern and Taconic aquafacies), or open ocean Iapetus waters (Holmden et al., 1998) that influenced nutrient concentrations and thus  $\delta^{13}\text{C}_{\text{org}}$ . Specifically, the more protracted fall in  $\Delta^{13}\text{C}$  values began at the peak of the GICE (Fig. 7), when compared to Pennsylvania and China (Fig. 11), is interpreted to reflect a lowering of growth rates in waters stripped of nutrients in nearby regions. This is consistent with the inferred direction of surface water currents flowing from northeast to southwest over eastern North America in the Upper Ordovician (Wilde, 1991; Kolata et al., 2001). In order to explain the different  $\Delta^{13}\text{C}$  trends between West Virginia and Pennsylvania, growth rates had to be higher in West Virginia before the GICE peak and then lower afterwards (Figs. 10 and 11). Alternatively, the unique West Virginia trends could reflect locally higher concentrations of  $\text{CO}_2(\text{aq})$  in seawater from this deeper water setting that was closer to the axis of foreland basin relative to the Salona and Coburn Formations of Pennsylvania (Diecchio, 1986; Fichter and Diecchio, 1986; Slupik, 1999). Further detailed sedimentologic, biostratigraphic, and compound-specific isotope work is needed to determine the exact cause(s) of the unique  $\Delta^{13}\text{C}$  trend from West Virginia.

## 6. Implications and conclusions

The paired  $\delta^{13}\text{C}_{\text{carb}}$  and  $\delta^{13}\text{C}_{\text{org}}$  trends from the Pagoda Formation of south China are similar to previously documented records from Pennsylvania and Iowa (Patzkowsky et al., 1997; Pancost et al., 1999) and possibly record a global trend that is linked to changes in atmospheric  $\text{CO}_2$  levels during the GICE. This represents the first evidence of a global change in  $\Delta^{13}\text{C}$ , consistent with the notion that global cooling began in the early Katian (e.g., Pope and Steffen, 2003; Saltzman and Young, 2005).

The  $\Delta^{13}\text{C}$  trends from Oklahoma and West Virginia are interpreted to reflect local decreases in marine phytoplankton growth rates that

overwhelmed the influence of a global drop in atmospheric  $p\text{CO}_2$  through the GICE (Fig. 10; Hayes et al., 1999; Joachimski et al., 2002). In Oklahoma, the inferred drop in phytoplankton growth rates is coincident with lithologic evidence for changes in nutrient input associated with the change from upwelling (eutrophic surface waters) to downwelling (oligotrophic surface waters). This change in oceanography could be attributed to shift in the site of deep water formation (from high to low latitudes) associated with a shift in climatic states, and this paleoceanographic model has been proposed for some Silurian  $\delta^{13}\text{C}$  excursions (e.g., Jeppsson, 1990; Cramer and Saltzman, 2007). In West Virginia, the  $\Delta^{13}\text{C}$  offset compared to the global pattern is less significant than in Oklahoma, and was likely due to advection of adjacent surface water masses that had been depleted in nutrients. This study demonstrates the importance of high-resolution paired  $\delta^{13}\text{C}_{\text{carb}}$  and  $\delta^{13}\text{C}_{\text{org}}$  from multiple sections worldwide in understanding the paleoceanographic conditions during fluctuations of the global carbon cycle.

## Acknowledgements

The stable isotope biogeochemistry laboratory (Andrea Grottole and Yohei Matsui) and the radiogenic isotope laboratory (Ken Foland and Jeff Linder) at the Ohio State University are gratefully acknowledged for sample analysis and technical support. We would also like to thank Brad Cramer for insightful discussion of an earlier version of this manuscript. We thank the two anonymous reviewers for their helpful and detailed comments that improved the manuscript. Funding for this project was provided by a National Science Foundation grant to M. Saltzman and K. Foland, and a Geological Society of America graduate student research grant to S. Young. This project was also partially supported by National Science Foundation grant EAR 0750726 to S. Leslie.

## References

- Ainsaar, L., Meidla, T., Martma, T., 1999. Evidence for a widespread carbon isotopic event associated with late Middle Ordovician sedimentological and faunal changes in Estonia. *Geological Magazine* 136, 49–62.
- Alberstadt, L.P., 1973. Articulate brachiopods of the Viola Formation (Ordovician) in the Arbuckle Mountains, Oklahoma. *Oklahoma Geological Survey Bulletin* 117, 1–87.
- An, T.-X., 1987. Early Paleozoic conodonts from south China. Beijing University Press, Beijing, 128 pp.
- Banner, J.L., Hanson, G.N., 1990. Calculation of simultaneous isotopic and trace element variations during water-rock interaction with applications to carbonate diagenesis. *Geochimica et Cosmochimica Acta* 54, 3123–3137.
- Bergström, S.M., Finney, S.C., Chen, X., Palsson, C., Wang, X.-F., Grahn, Y., 2000. A proposed global boundary stratotype for the base of the Upper Ordovician Series of the Ordovician System. *Episodes* 23, 102–109.
- Bergström, S.M., Saltzman, M.R., Schmitz, B., 2006. First record of the Hirnantian (Upper Ordovician)  $\delta^{13}\text{C}$  excursion in the North American Midcontinent and its regional implications. *Geological Magazine* 143, 657–678.
- Bergström, S.M., Chen, X., Schmitz, B., Young, S.A., Rong, J.-Y., Saltzman, M.R., in press. First documentation of the Ordovician Guttenberg  $\delta^{13}\text{C}$  excursion in Asia: Chemostratigraphy of the Pagoda and Yanwashan Formations in southeastern China. *Geological Magazine*, 16, 1–11. doi:10.1017/S0016756808005748.
- Bidigare, R.R., Fluegge, A., Freeman, K.H., Hanson, K.L., Hayes, J.M., Hollander, D., Jasper, J.P., King, L.L., Laws, E.A., Milder, J., Millero, F.J., Pancost, R., Popp, B.N., Steinberg, P.A., Wakeham, S.G., 1997. Consistent fractionation of  $^{13}\text{C}$  in nature and in the laboratory: growth-rate effects in some haptophyte algae. *Global Biogeochemical Cycles* 11, 279–292.
- Brenchley, P.J., Marshall, J.D., Carden, G.F., Robertson, D.B., Long, D.F., Meidla, T., Hints, L., Anderson, T.F., 1994. Bathymetric and isotopic evidence for a short-lived late Ordovician glaciation in a greenhouse period. *Geology* 22, 295–298.
- Brenchley, P.J., Carden, G.A.F., Hints, L., Kaljo, D., Marshall, J.D., Martma, T., Meidla, T., Nolvak, J., 2003. High-resolution stable isotope stratigraphy of Upper Ordovician sequences: Constraints on the timing of bioevents and environmental changes associated with mass extinction and glaciation. *Geological Society of America Bulletin* 115, 89–104.
- Chen, X., Rong, J.-Y., Wang, X.-F., Zhang, Z.-H., Zhang, Y.-D., Zhan, R.-B., 1995. Correlation of the Ordovician rocks of China. Chart and Explanatory Notes. International Union of Geological Sciences Publication 31, 1–104.
- Clayton, C.J., 1991. Effect of maturity on carbon isotope ratios of oils and condensates. *Organic Geochemistry* 17, 887–899.
- CLIMAP Project Members, 1981. Seasonal reconstruction of the Earth's surface at the last glacial maximum: Geological Society of America Map & Chart Series, MC-36.

- Cramer, B.D., Saltzman, M.R., 2007. Fluctuations in epeiric sea carbonate production during Silurian positive carbon isotope excursions: A review of proposed paleoceanographic models. *Palaeogeography, Palaeoclimatology, Palaeoecology* 245, 37–45.
- Diecchio, R.J., 1986. Taconian clastic sequence and general geology in the vicinity of the Allegheny Front in Pendleton County, West Virginia. In: Neathery, T.L. (Ed.), Southeastern Section of the Geological Society of America Centennial Field, vol. 6, pp. 85–90.
- Epstein, A.G., Epstein, J.B., Harris, L., 1977. Conodont color alteration—an index to organic metamorphism. U.S.G.S. Professional Paper 995, 1–27.
- Fanton, K.C., Holmden, C., 2007. Sea-level forcing of carbon isotope excursions in epeiric seas: implications for chemostratigraphy. *Canadian Journal of Earth Sciences* 44, 807–818.
- Fichter, L.S., Diecchio, R.J., 1986. The Taconic sequence in the northern Shenandoah Valley, Virginia. In: Neathery, T.L. (Ed.), Southeastern Section of the Geological Society of America Centennial Field 6, 73–78.
- Finney, S.C., 1986. Graptolite biofacies and correlation of eustatic, subsidence, and tectonic events in the Middle to Upper Ordovician of North America. *Palaios* 1, 435–461.
- Fischer, G., Müller, P.J., Wefer, G., 1998. Latitudinal  $\delta^{13}\text{C}_{\text{org}}$  variations in sinking matter and sediments from the South Atlantic: effects of anthropogenic  $\text{CO}_2$  and implications for paleo- $p\text{CO}_2$  reconstructions. *Journal of Marine Systems* 17, 471–495.
- Frakes, L.A., Francis, J.E., Syktus, J.I., 1992. Climate modes of the Phanerozoic. Cambridge University Press, Cambridge, pp. 15–26.
- Francois, R., Altabet, M.A., Goericke, R., McCorkle, D.C., Brunet, C., Poisson, A., 1993. Changes in the  $\delta^{13}\text{C}$  of surface water particulate organic matter across the subtropical convergence in the SW Indian Ocean. *Global Biogeochemical Cycles* 7, 627–644.
- Freeman, K.H., Hayes, J.M., 1992. Fractionation of carbon isotopes by phytoplankton and estimates of ancient  $\text{CO}_2$  levels. *Global Biogeochemical Cycles* 6, 185–198.
- Gao, G., Dworkin, S.I., Land, L.S., Elmore, R.D., 1996. Geochemistry of Late Ordovician Viola Limestone, Oklahoma: implications for marine carbonate mineralogy and isotopic compositions. *Journal of Geology* 104, 359–367.
- Goericke, R., Fry, B., 1994. Variations of marine plankton  $\delta^{13}\text{C}$  with latitude, temperature, and dissolved  $\text{CO}_2$  in the world ocean. *Global Biogeochemical Cycles* 8, 85–90.
- Goldman, D., Leslie, S.A., Nölvak, J., Young, S.A., Bergström, S.M., Huff, W.D., 2007. The Global Stratotype Section and Point (GSSP) for the base of the Katian Stage of the Upper Ordovician Series at Black Knob Ridge, Southeastern Oklahoma, USA. *Episodes* 30, 258–270.
- Gong, C., Hollander, D.J., 1997. Differential contribution of bacteria to sedimentary organic matter in oxic and anoxic environments, Santa Monica Basin, California. *Organic Geochemistry* 26, 545–563.
- Hatch, J.R., Jacobson, S.R., Witzke, B.J., Risatti, J.B., Anders, D.E., Watney, W.L., Newell, K.D., Vuletich, A.K., 1987. Possible late Middle Ordovician carbon isotope excursion: evidence from Ordovician oils and hydrocarbon source rocks, Mid-Continent and East-Central United States. *American Association of Petroleum Geologists Bulletin* 71, 1342–1354.
- Hayes, J.M., Popp, B.N., Takigiku, R., Johnson, M.W., 1989. An isotopic study of biogeochemical relationships between carbonates and organic carbon in the Greenhorn Formation. *Geochimica et Cosmochimica Acta* 53, 2961–2972.
- Hayes, J.M., Strauss, H., Kaufman, A.J., 1999. The abundance of  $^{13}\text{C}$  in marine organic matter and isotopic fractionation in the global biogeochemical cycle of carbon during the past 800 Ma. *Chemical Geology* 161, 103–125.
- Herrmann, A.D., Patzkowsky, M.E., Pollard, D., 2003. Oblivious forcing with 8–12 times preindustrial levels of atmospheric  $p\text{CO}_2$  during the Late Ordovician glaciation. *Geology* 31, 485–488.
- Herrmann, A.D., Haupt, B.J., Patzkowsky, M.E., Seidov, D., Slingerland, R.L., 2004. Response of Late Ordovician paleoceanography to changes in sea level, continental drift, and atmospheric  $p\text{CO}_2$ : potential causes for long-term cooling and glaciation. *Palaeogeography, Palaeoclimatology, Palaeoecology* 210, 385–401.
- Hinga, K.R., Arthur, M.A., Pilson, M.E.Q., Whitaker, D., 1994. Carbon isotope fractionation by marine phytoplankton in culture: the effects of  $\text{CO}_2$  concentration, pH, temperature, and species. *Global Biogeochemical Cycles* 8, 91–102.
- Holland, S.M., Patzkowsky, M.E., 1996. Sequence stratigraphy and long-term paleoceanographic change in the Middle and Upper Ordovician of the eastern United States. *Geological Society of America Special Paper* 306, 117–129.
- Holmden, C., Creaser, R.A., Muehlenbachs, K., Leslie, S.A., Bergström, S.M., 1998. Isotopic evidence for geochemical decoupling between ancient epeiric seas and bordering oceans: Implications for secular curves. *Geology* 26, 567–570.
- Jahren, A.H., Porter, S., Kuglitsch, J.J., 2003. Lichen metabolism identified in Early Devonian terrestrial organisms. *Geology* 31, 99–102.
- Jeppsson, L., 1990. An oceanic model for lithological and faunal changes tested on the Silurian record. *Journal of the Geological Society (London)* 147, 663–674.
- Joachimski, M.M., Pancost, R.D., Freeman, K.H., Ostertag-Henning, C., Buggisch, W., 2002. Carbon isotope geochemistry of the Frasnian–Famennian transition. *Palaeogeography, Palaeoclimatology, Palaeoecology* 181, 91–109.
- Kaljo, D., Martma, T., Saadre, T., 2007. Post-Hunnebergian Ordovician carbon isotope trend in Baltoscandia, its environmental implications and some similarities with that of Nevada. *Palaeogeography, Palaeoclimatology, Palaeoecology* 245, 138–155.
- Keith, C., 1989. Conodonts and Conodont Biostratigraphy of the Dolly Ridge Formation in Virginia and West Virginia. Unpublished B. S. Thesis, University of North Carolina, Wilmington, NC, 47 pp.
- Kienast, M., Calvert, S.E., Pelejero, C., Grimalt, J.O., 2001. A critical review of marine sedimentary  $\delta^{13}\text{C}_{\text{org}}$ - $p\text{CO}_2$  estimates: New palaeorecords from the South China Sea and a revisit of other low-latitude  $\delta^{13}\text{C}_{\text{org}}$ - $p\text{CO}_2$  records. *Global Biogeochemical Cycles* 15, 113–127.
- Kolata, D.R., Huff, W.D., Bergström, S.M., 2001. The Ordovician Seabee trough: an oceanic passage to the Midcontinent United States. *Geological Society of America Bulletin* 113 (8), 1067–1078.
- Kump, L.R., Arthur, M.A., 1999. Interpreting carbon-isotope excursions: carbonates and organic matter. *Chemical Geology* 161, 181–198.
- Laarkamp, K.L., Raymo, M.E., 1995. Carbon isotopic composition of particulate organic matter from the interior of the Equatorial Pacific Ocean. ICP V Program and Abstracts, 5th International Conference on Paleoceanography. University of New Brunswick, Fredericton. 132 p.
- Laws, E.A., Popp, B.N., Bidigare, R.R., Kennicutt, M.C., Macko, S.A., 1995. Dependence of phytoplankton carbon isotopic composition on growth rate and  $[\text{CO}_2]_{\text{aq}}$ : theoretical considerations and experimental results. *Geochimica et Cosmochimica Acta* 59, 1131–1138.
- Leslie, S.A., Bergström, S.M., 1997. Use of K-bentonite beds as time-planes for high-resolution lithofacies analysis and assessment of net rock accumulation rate: An example from the upper Middle Ordovician of eastern North America. *Geological Society of America Special Paper* 321, 11–21.
- Long, D.G.F., 1993. Oxygen and carbon isotopes and event stratigraphy near the Ordovician–Silurian boundary, Anticosti Island, Quebec. *Palaeogeography, Palaeoclimatology, Palaeoecology* 104, 49–59.
- Ludvigson, G.A., Jacobson, S.R., Witzke, B.J., González, L.A., 1996. Carbonate component chemostratigraphy and depositional history of the Ordovician Decorah Formation, Upper Mississippi Valley. In: Witzke, B.J., Ludvigson, G.A., Day, J. (Eds.), *Paleozoic Sequence Stratigraphy: views from the North American Craton*. Geological Society of America Special Paper, vol. 306, pp. 67–86.
- Männik, P., Vira, V., 2005. Distribution of Ordovician conodonts. In: Pöldvere, A. (Ed.), *Estonian Geological Sections. Mehikoorma (421) Drill Core*. Geological Survey of Estonia Bulletin 6, pp. 16–20.
- Marshall, J.D., Middleton, P.D., 1990. Changes in marine isotopic composition and the late Ordovician glaciation. *Journal of the Geological Society (London)* 147, 1–4.
- Melchin, M.J., Holmden, C., 2006. Carbon Isotope chemostratigraphy in Arctic Canada: Sea-level forcing of carbonate platform weathering and implications for Hirnantian global correlation. *Palaeogeography, Palaeoclimatology, Palaeoecology* 234, 186–200.
- Nowlan, G.S., Barnes, C.R., 1987. Application of conodont colour alteration indices to regional and economic geology. In: Austin, R.L. (Ed.), *Conodonts: Investigative Techniques and Applications*. Ellis Horwood Limited, Chichester, pp. 188–202.
- Pagani, M., Arthur, M.A., Freeman, K.H., 1999. Miocene evolution of atmospheric carbon dioxide. *Paleoceanography* 14, 273–292.
- Panchuk, K.M., Holmden, C.M., Leslie, S.A., 2006. Local controls on carbon cycling in the Ordovician midcontinent region of North America, with implications for carbon isotope secular curves. *Journal of Sedimentary Research* 76, 200–211.
- Pancost, R.D., Freeman, K.H., Patzkowsky, M.E., 1999. Organic-matter source variation and the expression of a late Middle Ordovician carbon isotope excursion. *Geology* 27, 1015–1018.
- Patzkowsky, M.E., Holland, S.M., 1993. Biotic response to a Middle Ordovician paleoceanographic event in eastern North America. *Geology* 21, 619–622.
- Patzkowsky, M.E., Slupik, L.M., Arthur, M.A., Pancost, R.D., Freeman, K.H., 1997. Late Middle Ordovician environmental change and extinction: harbinger of the Late Ordovician or continuation of Cambrian patterns? *Geology* 25, 911–914.
- Perry Jr., W.J., 1972. The Trenton Group of Nittany Anticlinorium, eastern West Virginia. *West Virginia Geological and Economic Survey Circular* 13, 1–28.
- Pope, M.C., 2004. Cherty carbonate facies of the Montoya Group, southern New Mexico and western Texas and its regional correlatives: a record of Late Ordovician paleoceanography on southern Laurentia. *Palaeogeography, Palaeoclimatology, Palaeoecology* 210, 367–384.
- Pope, M.C., Read, J.F., 1998. Ordovician meter-scale cycles: implications for climate and eustatic fluctuations in the central Appalachians during a global greenhouse, non-glacial to glacial transition. *Palaeogeography, Palaeoclimatology, Palaeoecology* 138, 27–42.
- Pope, M.C., Steffen, J.B., 2003. Widespread, prolonged late Middle to Late Ordovician upwelling in North America: a proxy record of glaciation? *Geology* 31, 63–66.
- Popp, B.N., Laws, E.A., Bidigare, R.R., Dore, J.E., Hanson, K.L., Wakeham, S.G., 1998. Effect of phytoplankton cell geometry on carbon isotopic fractionation. *Geochimica et Cosmochimica Acta* 62, 69–77.
- Rau, G.H., Takahashi, T., Marais, D.J.D., 1989. Latitudinal variations in plankton  $\delta^{13}\text{C}$ : implications for  $\text{CO}_2$  and productivity in past oceans. *Nature* 341, 516–518.
- Richardson, J.G., Ausich, W.I., 2007. Late Ordovician–Early Silurian cryptospore occurrences on Anticosti Island, Quebec, Canada. *Canadian Journal of Earth Sciences* 44, 1–7.
- Richardson, J.G., Bergström, S.M., 2003. Regional stratigraphic relations of the Trenton Limestone (Chatfieldian, Ordovician) in the eastern North American Midcontinent. *Northeastern Geology and Environmental Sciences* 18, 93–115.
- Romanek, C.S., Grossman, E.L., Morse, J.W., 1992. Carbon isotopic fractionation in synthetic aragonite and calcite: Effects of temperature and precipitation rate. *Geochimica et Cosmochimica Acta* 56, 419–430.
- Rosenau, N.A., Leslie, S.A., Herrmann, A., 2007. Sea surface temperature change from Late Ordovician  $\delta^{18}\text{O}$  data, Bromide and Viola Springs Formations, Oklahoma, USA. *Abstracts with Programs–Geological Society of America* 39 (6), 15.
- Royer, D.L., Berner, R.A., Beerling, D.J., 2001. Phanerozoic  $\text{CO}_2$  change: evaluating geochemical and paleobiological approaches. *Earth-Science Reviews* 54, 349–392.
- Saltzman, M.R., 2002. Carbon isotope ( $\delta^{13}\text{C}$ ) stratigraphy across the Silurian–Devonian transition in North America: evidence for a perturbation of the global carbon cycle. *Palaeogeography, Palaeoclimatology, Palaeoecology* 187, 83–100.
- Saltzman, M.R., Young, S.A., 2005. A long-lived glaciation in the Late Ordovician?: Isotopic and sequence-stratigraphic evidence from western Laurentia. *Geology* 33, 109–112.
- Saltzman, M.R., Brasier, M.D., Ripperdan, R.L., Ergaliev, G.K., Lohmann, K.C., Robinson, R.A., Chang, W.T., Peng, S., Runnegar, B., 2000. A global carbon isotope excursion

- (SPICE) during the Late Cambrian: relation to trilobite extinctions. *Palaeogeography, Palaeoclimatology, Palaeoecology* 162, 211–223.
- Saltzman, M.R., Bergström, S.M., Huff, W.D., Kolata, D.R., 2003. Conodont and graptolite Biostratigraphy and the Ordovician (early Chatfieldian, Middle Caradocian)  $\delta^{13}\text{C}$  Excursion in North America and Baltoscandia: implications for the Interpretations of the relations between the Millbrig and Kinnekulle K-bentonites. In: Albanesi, G.L., Beresi, M.S., Peralta, S.H. (Eds.), *Ordovician from the Andes*, vol. 17. Instituto Superior De Correlacion Geologica (Insugeo), Serie Correlacion Geologica, pp. 137–142.
- Scotese, C.R., McKerrow, W.S., 1991. Ordovician plate tectonic reconstructions. In: Barnes, C.R., Williams, S.H. (Eds.), *Advances in Ordovician Geology*, vol. 90–9. Geological Survey of Canada Paper, pp. 271–282.
- Slupik, L.M., 1999. Sedimentology and stable isotope chemostratigraphy of Late Middle Ordovician carbonates in central Pennsylvania. M. S. Thesis, Pennsylvania State University, State College, PA, 135 pp.
- Stemans, P., Wellman, C.H., 2004. Miospores and the emergence of Land Plants. In: Webby, B.D., Paris, F., Droser, M.L., Percival, I.G. (Eds.), *The Great Ordovician Biodiversification Event*. Columbia Press, New York, pp. 361–366.
- Strother, P.K., Al-Hajri, S., Traverse, A., 1996. New evidence for land plants from the lower Middle Ordovician of Saudi Arabia. *Geology* 24, 55–59.
- Sweet, W.C., 1983. Conodont Biostratigraphy of Fite Formation and Viola Group. Oklahoma Geological Survey Bulletin 132, 23–36.
- Tobin, K.J., Bergström, S.M., De La Garza, P., 2005. A mid-Caradocian (453 Ma) drawdown in atmospheric  $\text{pCO}_2$  without ice sheet development? *Palaeogeography, Palaeoclimatology, Palaeoecology* 226, 187–204.
- Valek, K.W., 1982. Conodont biostratigraphy of the Salona and Coburn Formations in the Middle Ordovician of central Pennsylvania. Unpublished M.S. thesis, The Ohio State University, Columbus, OH, 70 pp.
- Wilde, P., 1991. Oceanography in the Ordovician. In: Barnes, C.R., Williams, S.H. (Eds.), *Advances in Ordovician Geology*, vol. 90–9. Geological Survey of Canada Paper, pp. 283–298.
- Witzke, B.J., 1990. Palaeoclimatic constraints for Paleozoic paleolatitudes of Laurentia and Euramerica. In: McKerrow, W.S., Scotese, C.R. (Eds.), *Palaeogeography and Biogeography*. Geological Society Memoir, vol. 12, pp. 57–73.
- Young, S.A., Saltzman, M.R., Bergström, S.M., 2005. Upper Ordovician (Mohawkian) carbon isotope ( $\delta^{13}\text{C}$ ) stratigraphy in eastern and central North America: Regional expression of a perturbation of the global carbon cycle. *Palaeogeography, Palaeoclimatology, Palaeoecology* 222, 53–76.